of product quality for autologous transplantation because of the lack of quantitative analysis and non-human estimation as well as patient dependence. Thus, it is necessary to create a method that is suitable for *in vitro* quantitative estimation of the transplants.

In a previous study, a five-layered human skeletal muscle myoblast (HSMM) sheet was constructed to determine sheet fluidity by confocal laser scanning microscopy with image processing [10]. In the present study, an *in vitro* system based on a multilayered HSMM sheet with human umbilical vein endothelial cells (HUVECs) was developed to mimic the *in vivo* angiogenesis in the HSMM sheet after transplantation. Image processing was performed to evaluate the HUVEC spatial distribution and network formation in the HSMM sheet to elucidate the spatial habitation arising from HUVEC migration and connection.

2. Materials and methods

2.1. Cell preparation

HSMMs (Lot. No. 4F1618; Lonza Walkersville Inc., Walkersville, MD) and HUVECs (Lot. No. 4F0709; Lonza Walkersville Inc.) were used in the experiments. According to procedures described elsewhere [11], subcultures of HSMMs on laminin-coated surfaces were conducted at 37 °C in an atmosphere of 5% CO_2 in Dulbecco's Modified Eagle's Medium (DMEM; Sigma–Aldrich, St. Louis, MO) containing 10% fetal bovine serum (FBS; Invitrogen, Grand Island, NY) and antibiotics (100 U/cm^3 penicillin G, 0.1 mg/cm^3 streptomycin, and 0.25 mg/cm^3 amphotericin B; Invitrogen). HUVECs were cultured in a commercially available medium (EGM-2; Lonza Walkersville Inc.). The medium depth was set to 2 mm throughout the experiments.

2.2. Incubation of five-layered HSMM sheet with HUVECs

Five-layered HSMM sheet was fabricated according to a previously reported method [10]. In brief, as shown in Fig. 1A, starter HSMMs prepared by subculturing were stained with CellTracker™ Orange (Invitrogen) to obtain fluorescent orange cells according to a commercially recommended protocol (5 μM for 15 min for live cell imaging). The HSMMs were seeded at 2.3 × 10^5 cells/cm^2 in each well (1.9 cm^2) of 24-well UpCell™ plates (CellSeed, Tokyo, Japan) with a temperature-responsive surface grafted with PNIPAAm and incubated for 24 h at 37 °C in a 5% CO_2 atmosphere to form the monolayer sheet. To stack monolayer sheets to fabricate the multilayered cell sheet, the customized stamps with the gelatin gel (G1890-100G; Sigma–Aldrich) were used. To harvest the monolayer sheet, the stamp with the gelatin gel was overlaid on the monolayer sheet in a well at 37 °C, and the temperature was shifted to 20 °C. After 30 min, the stamp was lifted together with the monolayer sheet from the bottom surface of the well. The steps were then repeated for the sequential harvests of monolayer sheets to form the multilayered construct on the stamp. The multilayered sheet with the gelatin was peeled from the stamp for transfer to a dish containing the precultured HUVECs. For the preculture, HUVECs were seeded into culture dishes (35 mm in diameter; Corning Inc., NY) and cultured in the EGM-2 medium for 24 h. The initial density of HUVECs (X_0) for the subsequent incubation with the sheet was set in the range of 0.35–3.32 × 10^4 cells/cm^2 by changing the seeding density of HUVECs (X_s). The relationship between X_s and X_0 was determined in advance (Supplementary Table 1). After incubation at 20 °C for 2 h, the sheet was incubated at 37 °C in DMEM containing 10% FBS for 1 h to remove the gelatin. The medium containing the dissolved gelatin was exchanged with fresh medium. At the given incubation time (t), triplicate samplings were performed for quantitative analysis. During the incubation period, the medium was renewed every day.

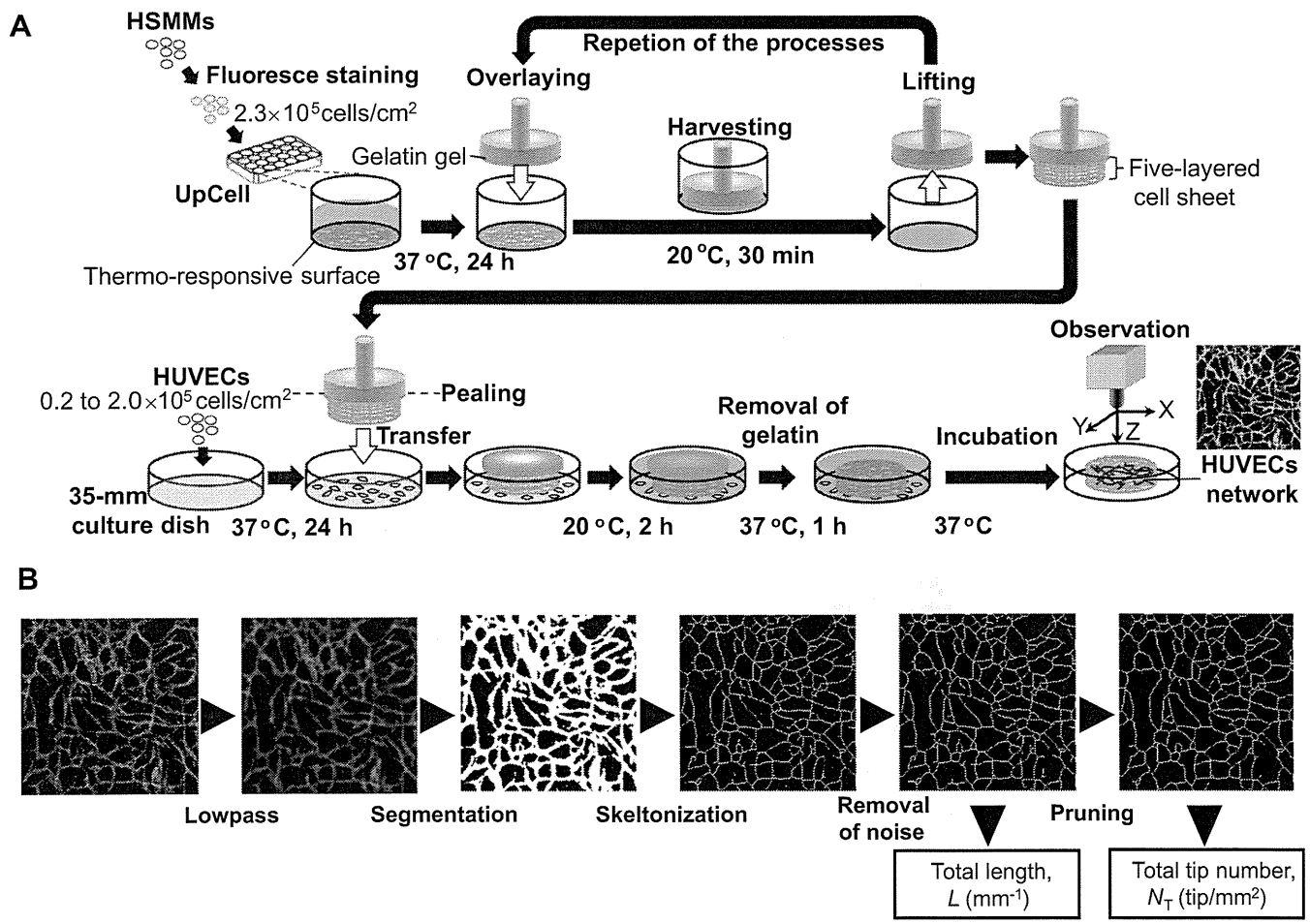

Fig. 1. Schematic drawings of experimental procedures. A: Construction of multilayered HSMM sheet and incubation with HUVECs. B: Image process procedure to evaluate HUVEC network formation and maturation.

2.3. Immunostaining for HUVECs

The culture system containing the five-layered HSMM sheet with HUVECs was washed with phosphate-buffered saline (PBS) and fixed in PBS containing 4% paraformaldehyde (Wako Pure Chemical Industries, Osaka, Japan) overnight. The fixed specimen was then permeabilized in PBS containing 0.1% Triton X-100 (Wako Pure Chemical Industries) for 12 min, washed twice with PBS, and then blocked in 1% bovine serum albumin (BSA; Wako Pure Chemical Industries) in PBS for 1 h. The specimen was labeled with a primary antibody (monoclonal mouse anti-human CD31 antibody; DAKO, Glostrup, Denmark) in 1% BSA solution overnight. The specimen was then thoroughly washed with PBS and immersed in 1% BSA solution containing the secondary antibody conjugated with Alexa Fluor® 488 (Invitrogen) for 1 h.

2.4. Evaluation of the HUVEC network formed inside the HSMM sheet

The image capture was carried out using a 10× objective lens of confocal laser scanning microscope (FV-300; Olympus, Tokyo, Japan) at more than 8 positions in each sample. As shown in Fig. 1B, each image was 8-bit gray scale with a size of 256 × 256 pixels and covered an area of 942 × 942 μm. The images were subjected to image processing (Image-Pro Plus; Media Cybernetics Inc., Bethesda, MD) using a low-pass filter for primary noise removal and binarization with a certain intensity threshold. The threshold intensity was determined as the average of the mode intensity and the automatic threshold intensity calculated with an Otsu adaptive threshold algorithm [12], which chooses the threshold to minimize the intra-class variance of the thresholded black and white pixels with an exhaustive search. The binary images were subjected to skeletonization to produce lined objects, the secondary noise removal with a size threshold to remove items with a size of less than 16 pixels, and the pruning of small branches in the objects. The total length of the network per image area (L; cm^{-1}), and the number of total tips of the network (N_T; tip/cm^2), were measured to estimate the extent of the HUVEC network (L/N_T; cm/tip). The tips existing at the edge of the image were not counted.

2.5. Spatial distribution of HUVECs and HSMMs in five-layered HSMM sheets

To determine the vertical distribution of the HUVECs inside the HSMM sheet, the green cells (HUVECs labeled with Alexa Fluor 488) and orange cells (HSMMs stained with CellTracker™ Orange) in each layer were observed and quantitatively analyzed as previously described [10] (Supplementary Fig. 1). The number of colored pixels in each slice was counted. The green and orange pixels in each slice were normalized using the maximum green and orange pixel values, respectively, found in all of the slice images. Slices possessing more than 10% of the colored pixels were regarded to exist inside the cell sheet, from which the vertical positions at the top and bottom of the five-layered sheet, and the sheet thickness, h (μm), were determined. The green pixels inside the sheet were normalized to determine the vertical distribution of the green pixels by dividing them into 5 layers. The normalized distribution of the green pixels was assumed to be equivalent to the distribution of green cells in the sheet, which was determined as the frequency of green cells, f_G (−), in each layer. For determination of the vertical distribution of the HSMMs, HSMMs stained with CellTracker™ Green (Invitrogen) were placed in the bottom layer of a five-layered HSMM sheet, and their vertical distribution at 24 h was determined.

3. Results

3.1. HUVEC network formation inside the HSMM sheet

The behavior of HUVECs in the five-layered HSMM sheet was observed for 120 h to estimate the growth and network formation according to the parameters L, N_T, and L/N_T. The initial density of HUVECs was set at $X_0 = 1.29 \times 10^4$ cells/cm^2. At the beginning of the incubation period ($t = 0$), as shown in Fig. 2, the HUVECs were observed to be single and round-shaped with podia. At $t = 24$ h,

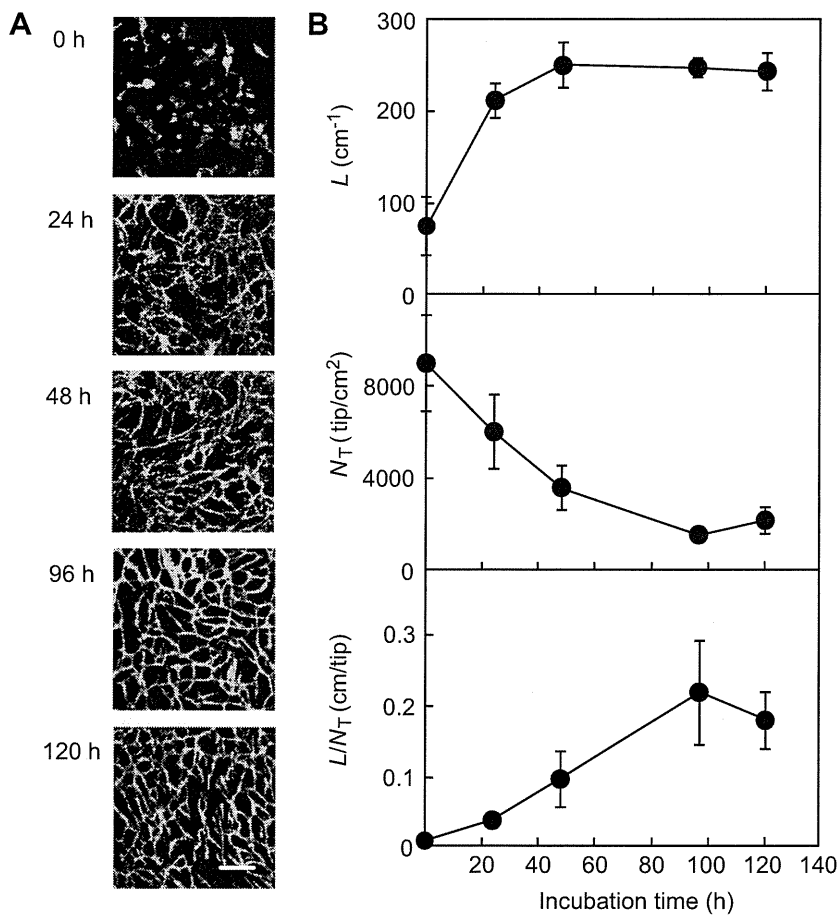

Fig. 2. Time course of HUVEC network formation inside the five-layered HSMM sheet at an initial HUVEC density (X_0) of 1.29 × 10^4 cells/cm^2. A: Horizontal images of HUVEC morphology. Scale bar: 200 μm. B: Evaluation of HUVEC network formation with image processing. L: total length (cm^{-1}), N_T: total tip number (tip/cm^2), L/N_T: extent of network formation (cm/tip). The bars show the standard deviation (SD) ($n = 3$).

most of the HUVECs were found to have elongated for initiation of migration in the sheet, resulting in an increase in L. With further prolongation of the incubation period beyond $t = 48$ h, the level of L was constant, i.e., the HUVECs did not grow further. In addition, the HUVECs began to encounter and connect with each other, resulting in a decrease in N_T until $t = 96$ h. Smooth connections of the HUVECs appeared at $t = 96$ h, which suggested the maturation of the HUVEC network. These behaviors were reflected by an increase in L/N_T although a slight decay of the connections occurred at $t = 120$ h. The maximum value of L/N_T was $= 0.22 \pm 0.07$ cm/tip at $t = 96$ h, which was 5.6 times higher than the value at $t = 24$ h.

3.2. Vertical migration of HUVECs during network formation

During network formation, the HUVECs were initially localized at the bottom of the HSMM sheet and then vertically migrated into the inner portion of the sheet to form aggregates with a lumen structure inside the sheet (Supplementary Fig. 2). To estimate the vertical migration of the HUVECs, their spatial distribution pattern was obtained as shown in Fig. 3. At the beginning ($t = 0$), the frequency of green cells (HUVECs) f_G was the highest in the first layer from the bottom surface, i.e., most of HUVECs were located at the bottom of the HSMM sheet. A broader distribution of f_G was obtained at $t = 24$ h, meaning the HUVEC migration toward the upper layers of sheet. In addition, the migration of the HUVECs was much faster than that of HSMMs because of the broader distribution of the HUVECs at $t = 24$ h (Supplementary Fig. 3). At $t = 96$ h, HUVECs inhabited the middle layer, with $f_G = 0.40$ and 0.30 in the second and third layers, respectively, which were higher than the values in the corresponding bottom and top layers. Fig. 3B and Supplementary movie 1 depict the aggregate shape of the HUVECs in the sheet at $t = 96$ h. The HUVECs in the middle layer formed a net-shaped aggregate to generate the network, whereas those in the top layer formed an island-shaped aggregate, which indicates that the shape of the HUVEC aggregate depended on their location in the sheet.

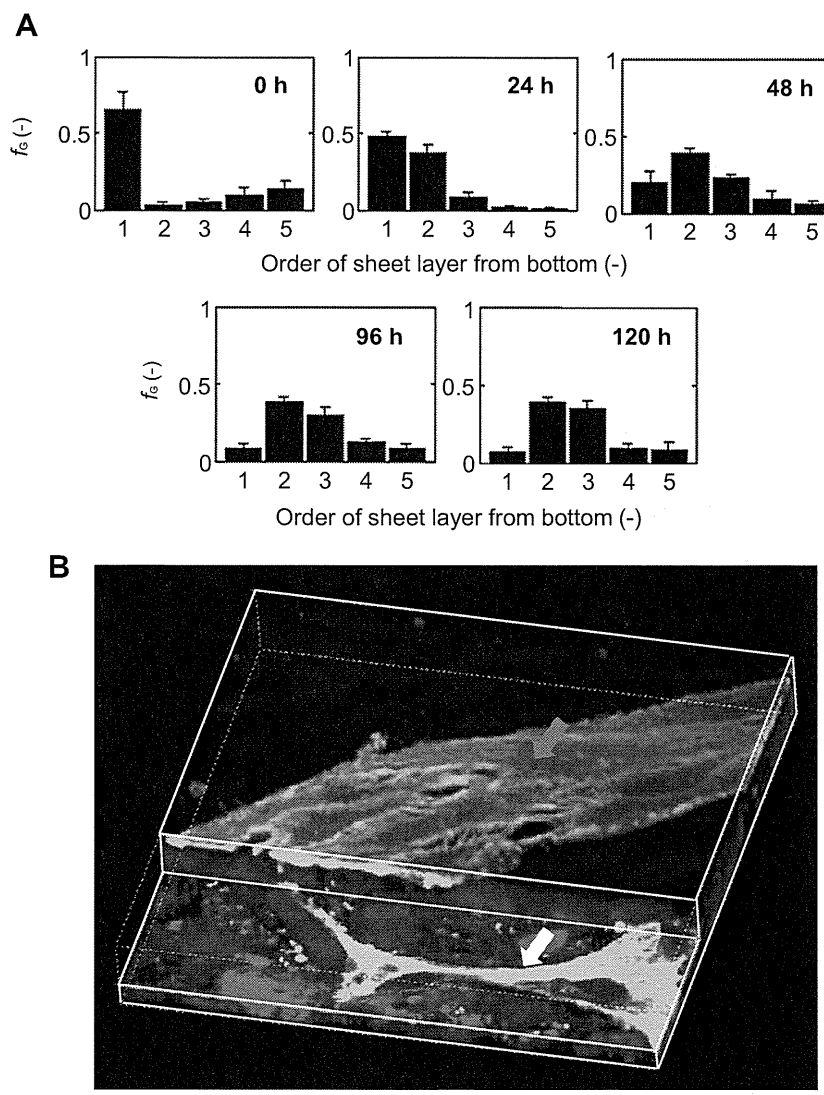

Fig. 3. Vertical analysis of HUVEC network formation inside the five-layered HSMM sheet at an initial HUVEC density (X_0) of 1.29×10^4 cells/cm^2. A: Time course of the spatial distribution of HUVECs (f_G) in each layer of the HSMM sheet. Bars show the standard deviation (SD) ($n = 3$). B: Three-dimensional image of HSMM sheet showing different shapes of HUVEC aggregates at different positions in/on the sheet at $t = 96$ h. The white arrow indicates net-shaped aggregation (network) in the middle layer of the cell sheet. The red arrow indicates island-shaped aggregation in the top layer on the cell sheet. (For interpretation of the references to colour in this figure legend, the reader is referred to the web version of this article.)

Supplementary video related to this article can be found at http://dx.doi.org/10.1016/j.biomaterials.2012.08.055.

3.3. Influence of HUVEC seeding density on migration and network formation

To evaluate the HUVEC connectivity in the sheet, the HUVECs were incubated for t = 96 h with initial densities ranging from $X_0 = 0.35 \times 10^4$ to 3.32×10^4 cells/cm^2. As shown in Fig. 4, with an increase in X_0, L/N_T increased to a maximum value of L/N_T = 0.484 cm/tip at $X_0 = 2.20 \times 10^4$ cells/cm^2, which was 2.3 times higher than the value at $X_0 = 1.29 \times 10^4$ cells/cm^2. In addition, the length and tip number of the HUVECs were estimated on the basis of the parameters such as specific length (L/X_0) and specific tip number (N_T/X_0), respectively. The L/X_0 and N_T/X_0 decreased with an increase in X_0 by $L/X_0 = 9.0 \times 10^{-3}$ cm/cell and $N_T/X_0 = 5.0 \times 10^{-2}$ tip/cell at $X_0 = 3.32 \times 10^4$ cells/cm^2, which were 3 and 30 times lower than the values at $X_0 = 0.35 \times 10^4$ cells/cm^2, respectively.

The f_G value of HUVECs at 96 h in the first, third, and fifth layers with respect to the initial density is shown in Fig. 5. In the fifth layer (top layer), with an increase in X_0, f_G decreased to 0.07 at $X_0 = 1.29 \times 10^4$ cells/cm^2, which was half of the value at $X_0 = 0.35 \times 10^4$ and 0.69×10^4 cells/cm^2. A further increase in X_0 resulted in a slight increase of f_G to 0.10 at $X_0 = 3.32 \times 10^4$ cells/cm^2. This trend was contrary to that observed in the third layer (middle layer).

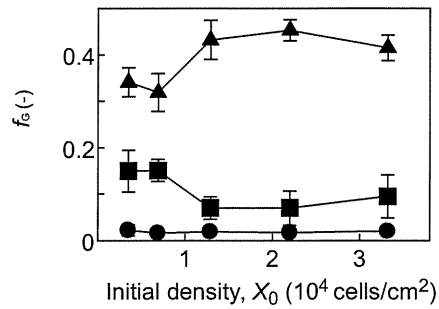

Fig. 5. Spatial distribution of HUVECs at 96 h with different initial densities of HUVECs (X_0) ranging from 0.35×10^4 to 3.32×10^4 cells/cm^2. Frequency of HUVECs (f_G) in the top (square), middle (triangle) and bottom (circle) layers are shown against X_0. Bars show the standard deviation (SD) (n = 3).

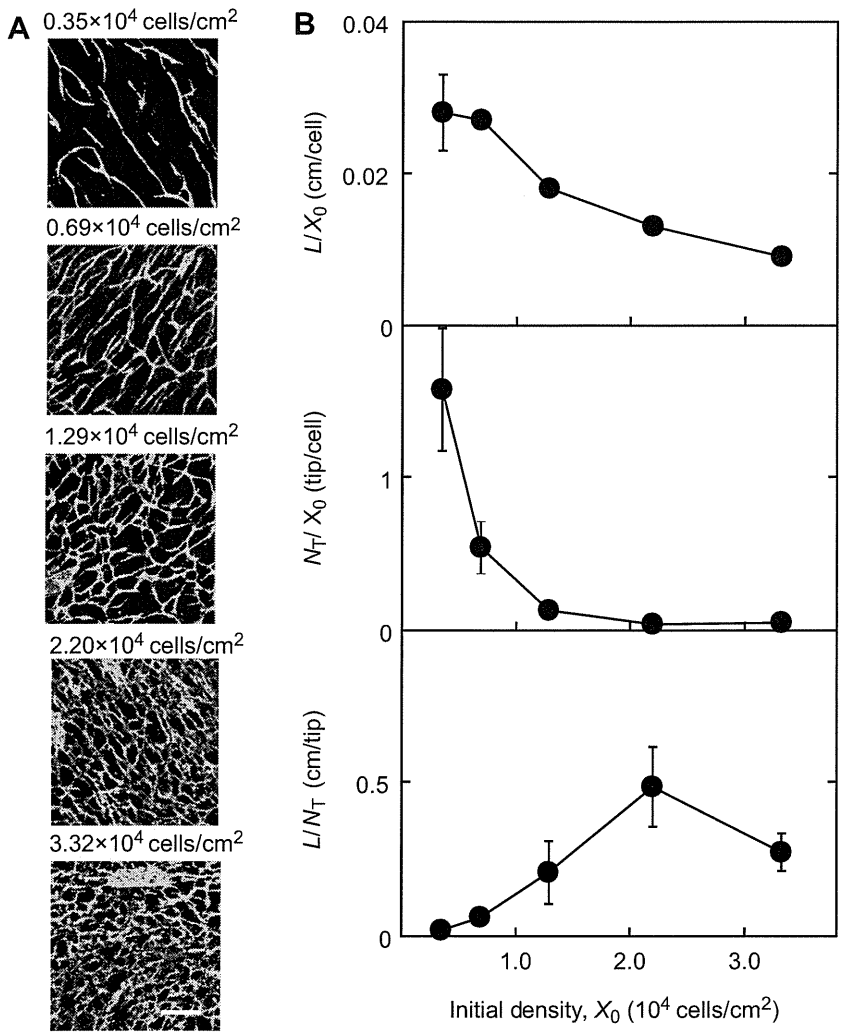

Fig. 4. Network formation at 96 h with different initial densities of HUVECs (X_0) ranging from 0.35×10^4 to 3.32×10^4 cells/cm^2. A: Horizontal images of HUVEC morphology. Scale bar: 200 μm. B: Evaluation of HUVEC network formation with image processing. L/X_0: specific length (cm/cell), N_T/X_0: specific tip number (tip/cell), L/N_T: extent of network formation (cm/tip). The bars show the standard deviation (SD) (n = 3).

4. Discussion

Cell migration in 3-D constructs plays an important role in physiological and pathological phenomena such as embryonic development, cell alignment, immune reactivity, angiogenesis, and metastasis [13]. Determining the mechanisms underlying cell migration in 3-D tissues having fluidity will be useful for designing biomimetic structures and functionally engineered tissues. Although the behaviors of cells on two-dimensional culture surfaces or in static 3-D scaffold have been extensively investigated, cell movement in fluidic 3-D tissues, especially vertical migration inside the tissue, has not been well addressed because of the absence of *in vitro* methods which enable quantitative and reproducible measurements. In the present study, a five-layered HSMM sheet was fabricated as a 3-D model to evaluate vertical cell migration by confocal laser scanning microscopy with image processing. We also established the mimic system of transplantation consisting of HUVECs on a culture dish that represents target cells at the lesion site as well as a five-layered HSMM sheet as the transplant tissue. This system can be used to model angiogenesis after transplantation. The HUVECs that were initially localized at the bottom of the HSMM sheet vertically migrated into the inner portion of the sheet. The migrating HUVECs encountered and connected with other HUVECs in the middle layer of the sheet to form a network (Figs. 2 and 3). In our previous study [10], the active fluidity by cellular migrations of HSMMs in the horizontal and vertical directions in the five-layered HSMM sheet was observed. The results of the present study revealed that the vertical migration of HUVECs was higher than that of HSMMs (Supplementary Fig. 3), demonstrating the active migration of HUVECs in a fluidic sheet.

The formation of HUVEC network regarded as a net-shaped aggregate was localized in the middle layer of the sheet owing to the encountering of HUVECs and their linear connections, while the unconnected HUVECs continued to migrate toward the top layer, forming the island-shaped aggregate (Fig. 3). These results show that the spatial habitation of HUVECs occurred in the top and middle layers of the sheet by their encountering and connection. In addition, the shape of the HUVEC aggregates depended on their location in the sheet. The further performance of HUVEC behavior at different densities supported the habitation (Figs. 4 and 5), revealing that the HUVECs were localized both in the middle and top layer at the low initial densities ($X_0 = 0.35 \times 10^4$ and 0.69×10^4 cells/cm^2), while only in the middle layer at the higher initial densities ($X_0 = 1.29 \times 10^4$ and 2.20×10^4 cells/cm^2). These results led to the mechanism for the spatial inhabitation as follows. As shown in Fig. 6, the frequency of encountering of HUVECs at a low concentration caused less connectivity in the middle layer of the sheet, and unconnected free HUVECs continued to migrate upward. With an increase in the HUVEC density in the sheet, the HUVECs exhibited a higher frequency of encountering to connect each other (at a moderate concentration). Excessive existence of HUVECs leads to less sites for their connection although higher frequency of encountering occurred, resulting in the larger number of HUVECs migrating toward top layer.

The dependence of the shape of the HUVEC aggregate on the location of the cells in the sheet was reported in previous studies. Asakawa et al. reported that HUVECs in multilayered sheet of human dermal fibroblasts formed a network with a tubular structure when the HUVECs were initially set in the middle layer of the sheet [14]. On the other hand, the introduction of HUVECs in the top layer of the sheet generated the island-shaped aggregates; thus the HUVEC habitation in the top and middle layers depended on the initial location of the HUVECs in the sheet. In the present study, the HUVECs outside the sheet did not grow in DMEM including 10% FBS due to no additional cytokines (data not shown). Thus, the network formation in the sheet could be attributed to the local feeding of cytokines from HSMMs. Candidate cytokines secreted from HSMMs are considered to be vascular endothelial growth factor, hepatocyte growth factor and fibroblast growth factor [15] which affect endothelial cell division, migration, and connection mediated by VE-cadherin expression [16–18].

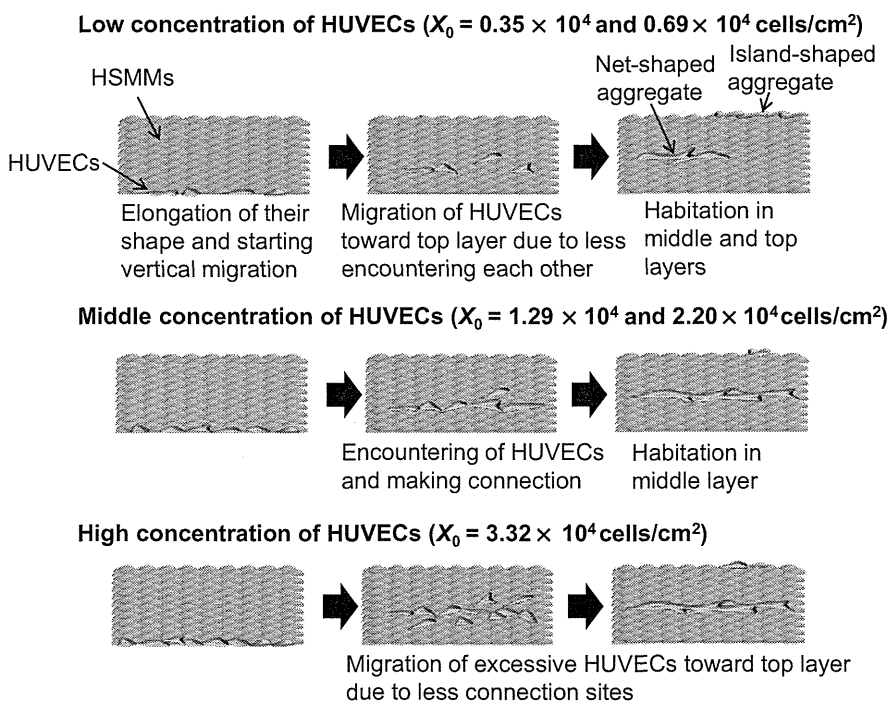

Fig. 6. Schematic illustration showing the probable behaviors of HUVECs in the HSMM sheet with various HUVEC initial densities.

The fabrication of aggregates, which is a minimum unit exhibiting tissue function, has been required to propose angiogenesis models [19]. A sphere-shaped aggregate is widely used as a platform for 3-D models or bio-mimic assay. However, histological analysis is necessary to evaluate the HUVEC network in the sphere-shaped aggregate, leading to a difficulty in observation [20–22]. Our system with a widespread HUVEC network in a multilayered sheet regarded as a plate-shaped aggregate enables the independent observation of the vertical and horizontal distributions of cells in 3-D constructs via one-dimensional (*Z*-axis) and two-dimensional (XY-axis) analyses, being a powerful tool for *in vitro* angiogenesis assays, which can evaluate the HUVEC behaviors such as migration, connection, as well as the formation of an endothelial network in a 3-D construct.

5. Conclusion

A five-layered HSMM sheet with HUVECs which mimic the *in vivo* transplantation system was developed. The HUVECs that were initially localized at the bottom of the HSMM sheet, exhibited vertical migration into the inner portions of the sheet, and formed networks in the middle layer of the sheet. The quantitative analysis of the vertical distribution of HUVECs in the sheet clarified the process of their network formation. Spatial habitation of the HUVEC network in the middle layer of the sheet was observed and the extent of the network formation depended on the frequency of encountering between HUVECs. Our system including widespread formation of HUVEC network in a fluidic scaffold and its evaluation method might be applicable not only for the *in vitro* construction of pre-vascularized tissue but also for *in vitro* angiogenesis models.

Acknowledgments

This study was supported by the New Energy and Industrial Technology Development Organization (NEDO) of Japan, the Japan Society for the Promotion of Science (JSPS) through the "Funding Program for World-Leading Innovative R&D on Science and Technology (FIRST Program)," initiated by the Council for Science and Technology Policy (CSTP), and Grant-in Aids for Scientific Research (Nos. 21360402 and 24360341) from Ministry of Education, Culture, Sports, Science and Technology.

Appendix A. Supplementary data

Supplementary data related to this article can be found at http://dx.doi.org/10.1016/j.biomaterials.2012.08.055.

References

[1] Haraguchi Y, Shimizu T, Sasagawa T, Sekine H, Sakaguchi K, Kikuchi T, et al. Fabrication of functional three-dimensional tissues by stacking cell sheets in vitro. Nat Protoc 2012;7:850–8.
[2] Okano T, Yamada N, Sakai H, Sakurai Y. A novel recovery-system for cultured-cells using plasma-treated polystyrene dishes grafted with poly(*N*-isopropylacrylamide). J Biomed Mater Res 1993;27:1243–51.
[3] Haraguchi Y, Shimizu T, Yamato M, Okano T. Scaffold-free tissue engineering using cell sheet technology. RSC Adv 2012;2:2184–90.
[4] Memon IA, Sawa Y, Fukushima N, Matsumiya G, Miyagawa S, Taketani S, et al. Repair of impaired myocardium by means of implantation of engineered autologous myoblast sheets. J Thorac Cardiovasc Surg 2005;130:1333–41.
[5] Miyagawa S, Roth M, Saito A, Sawa Y, Kostin S. Tissue-engineered cardiac constructs for cardiac repair. Ann Thorac Surg 2011;91:320–9.
[6] Sekine H, Shimizu T, Dobashi I, Matsuura K, Hagiwara N, Takahashi M, et al. Cardiac cell sheet transplantation improves damaged heart function via superior cell survival in comparison with dissociated cell injection. Tissue Eng Part A 2011;17:2973–80.
[7] Coppen SR, Fukushima S, Shintani Y, Takahashi K, Varela-Carver A, Salem H, et al. A factor underlying late-phase arrhythmogenicity after cell therapy to the heart – global downregulation of connexin43 in the host myocardium after skeletal myoblast transplantation. Circulation 2008;118:S138–44.
[8] Sawa Y, Miyagawa S, Sakaguchi T, Fujita T, Matsuyama A, Saito A, et al. Tissue engineered myoblast sheets improved cardiac function sufficiently to discontinue LVAS in a patient with DCM: report of a case. Surg Today 2012;42:181–4.
[9] Sekiya N, Matsumiya G, Miyagawa S, Saito A, Shimizu T, Okano T, et al. Layered implantation of myoblast sheets attenuates adverse cardiac remodeling of the infarcted heart. J Thorac Cardiovasc Surg 2009;138:985–93.
[10] Kino-oka M, Ngo TX, Nagamori E, Takezawa Y, Miyake Y, Sawa Y, et al. Evaluation of vertical cell fluidity in a multilayered sheet of skeletal myoblasts. J Biosci Bioeng 2012;113:128–31.
[11] Chowdhury SR, Muneyuki Y, Takezawa Y, Kino-oka M, Saito A, Sawa Y, et al. Growth and differentiation potentials in confluent state of culture of human skeletal muscle myoblasts. J Biosci Bioeng 2010;109:310–3.
[12] Otsu N. Threshold selection method from gray-level histograms. IEEE Trans Syst Man Cybern 1979;9:62–6.
[13] Horwitz R, Webb D. Cell migration. Curr Biol 2003;13:R756–9.
[14] Asakawa N, Shimizu T, Tsuda Y, Sekiya S, Sasagawa T, Yamato M, et al. Pre-vascularization of in vitro three-dimensional tissues created by cell sheet engineering. Biomaterials 2010;31:3903–9.
[15] Hawke TJ, Garry DJ. Myogenic satellite cells: physiology to molecular biology. J Appl Physiol 2001;91:534–51.
[16] Esser S, Lampugnani MG, Corada M, Dejana E, Risau W. Vascular endothelial growth factor induces VE-cadherin tyrosine phosphorylation in endothelial cells. J Cell Sci 1998;111:1853–65.
[17] Lamalice L, Le Boeuf F, Huot J. Endothelial cell migration during angiogenesis. Circ Res 2007;100:782–94.
[18] Underwood PA, Bean PA, Gamble JR. Rate of endothelial expansion is controlled by cell:cell adhesion. Int J Biochem Cell Biol 2002;34:55–69.
[19] Levenberg S, Rouwkema J, Macdonald M, Garfein ES, Kohane DS, Darland DC, et al. Engineering vascularized skeletal muscle tissue. Nat Biotechnol 2005;23:879–84.
[20] Kunz-Schughart LA, Schroeder JA, Wondrak M, van Rey F, Lehle K, Hofstaedter F, et al. Potential of fibroblasts to regulate the formation of three-dimensional vessel-like structures from endothelial cells in vitro. Am J Physiol Cell Physiol 2006;290:C1385–98.
[21] Rouwkema J, de Boer J, Van Blitterswijk CA. Endothelial cells assemble into a 3-dimensional prevascular network in a bone tissue engineering construct. Tissue Eng 2006;12:2685–93.
[22] Timmins NE, Dietmair S, Nielsen LK. Hanging-drop multicellular spheroids as a model of tumour angiogenesis. Angiogenesis 2004;7:97–103.

Circulation Journal
Official Journal of the Japanese Circulation Society
http://www.j-circ.or.jp

ORIGINAL ARTICLE
Cardiovascular Surgery

Predictor of Early Mortality for Severe Heart Failure Patients With Left Ventricular Assist Device Implantation

– Significance of INTERMACS Level and Renal Function –

Daisuke Yoshioka, MD; Taichi Sakaguchi, MD, PhD; Shunsuke Saito, MD; Shigeru Miyagawa, MD, PhD; Hiroyuki Nishi, MD; Yasushi Yoshikawa, MD; Satsuki Fukushima, MD, PhD; Tetsuya Saito, MD; Takashi Daimon, PhD; Takayoshi Ueno, MD, PhD; Toru Kuratani, MD, PhD; Yoshiki Sawa, MD, PhD

Background: The preoperative risk factors for left ventricular assist device (LVAD) implantation and their impact on the clinical outcome was analyzed to evaluate the optimal timing of LVAD implantation for severe heart failure patients.

Methods and Results: From January 2006 to August 2011, 82 patients underwent 84 LVAD implantations at the Osaka University Hospital. These patients were categorized into 2 groups: Interagency Registry for Mechanically Assisted Circulatory Support (INTERMACS) level 1 (n=41) and INTERMACS level 2/3 (n=43). The preoperative characteristics, early mortality, and cumulative survival between the 2 groups was compared. Ten (24.4%) patients died within 90 days in the INTERMACS level 1 group (multiple organ failure: 6, cerebrovascular event: 3, sepsis: 1), whereas 1 (2.3%) patient died because of a cerebrovascular event in the INTERMACS level 2/3 group (P=0.003). The cumulative survival rate was 82.9% at 30 days, 75.6% at 90 days, and 63.7% after 1 year in the INTERMACS level 1 group, and 100%, 97.7%, and 85.3% in the level 2/3 group (P=0.015). Using multivariate analysis for the INTERMACS level 1 group data, the preoperative serum creatinine level was the independent predictor of 90-day mortality.

Conclusions: LVAD implantation in a stable condition contributes to better clinical outcome for severe heart failure patients. If critical cardiogenic shock occurs, LVAD implantation must be considered immediately before other organs' functions, especially renal function, deteriorate. (*Circ J* 2012; **76:** 1631–1638)

Key Words: Heart failure; Left ventricular assist device; INTERMACS

Left ventricular assist devices (LVADs) provide effective bridge-to-transplant therapy for patients with end-stage heart failure and are being frequently used in destination therapy.[1–6] The number of patients undergoing LVAD implantation has increased considerably worldwide. In the past decade, several types of continuous-flow implantable devices have been developed, and they have demonstrated significantly improved clinical results with reduced pump-related morbidity and improved overall survival and quality of life for patients.[7–9]

Editorial p1587

The Interagency Registry for Mechanically Assisted Circulatory Support (INTERMACS), a National Heart Lung and Blood Institute (NHLBI)-sponsored collaborative database, has been maintaining records of durable mechanical circulatory support device implantation in the USA since 2006.[10,11] The INTERMACS's profiles of LVAD implantation are defined from level 1 to level 7, depending on patient severity (Table 1). In the second annual report from INTERMACS, which enrolled more than 1,000 patients, the survival rate categorized according to INTERMACS criteria showed early increased death for patients in level 1 (critical cardiogenic shock) at the time of LVAD implantation.[12]

However, there are still many patients referred for LVAD implantation who are categorized in the INTERMACS level 1 group, and the risk factors in these patients have not been fully

Received December 12, 2011; revised manuscript received February 20, 2012; accepted March 8, 2012; released online April 7, 2012
Time for primary review: 24 days
Department of Cardiovascular Surgery, Osaka University Graduate School of Medicine, Suita (D.Y., T. Sakaguchi, S.S., S.M., H.N., Y.Y., S.F., T. Saito, T.U., T.K., Y.S.); Department of Biostatics, Hyogo Medical College, Nishinomiya (T.D.), Japan
Grant: none.
Meeting Presentation: The 75th annual scientific meeting of the JCS, August 3rd–4th, Yokohama, Japan.
Mailing address: Yoshiki Sawa, MD, Department of Cardiovascular Surgery, Osaka University Graduate School of Medicine, 2-2 Yamadaoka, Suita 565-0871, Japan. E-mail: sawa@surg1.med.osaka-u.ac.jp
ISSN-1346-9843 doi:10.1253/circj.CJ-11-1452

Table 1. Interagency Registry for Mechanically Assisted Circulatory Support (INTERMACS)

Level	
1	Critical cardiogenic shock (Crush and Burn)
2	Progressive decline on inotropic support
3	Stable but inotropic dependent
4	Resting symptoms home on oral therapy
5	Exertion intolerant
6	Exertion limited
7	Advanced NYHA Class III symptoms

evaluated. In this study, we analyzed the clinical results of LVAD implantation with regard to the preoperative INTERMACS level and risk factors to evaluate the optimal timing of LVAD implantation for patients with severe heart failure.

Methods

Patients

Since the first continuous flow LVAD implantation at the Osaka University Hospital was performed in 2006, we enrolled 82 patients who underwent 84 LVAD implantations from January 2006 to August 2011. LVAD implantation was indicated for patients with irreversible end-stage heart failure who were eligible for, or possible candidates, for heart transplantation, with the exception of 1 patient who underwent Nipro LVAD implantation followed by a conversion to Jarvik 2000 (Jarvik Heart, Inc, New York, NY, USA) LVAD implantation as part of their destination therapy.[13] The hospital records of these 84 patients were retrospectively reviewed and categorized on the basis of their preoperative status according to INTERMACS level classification[10] as follows. INTERMACS level 1 included patients with life-threatening hypotension despite rapidly escalating inotropic support and critical organ hypoperfusion, often confirmed by worsening acidosis and/or lactate levels. INTERMACS level 2 included those unable to tolerate inotropic therapy, while level 3 patients had stable blood pressure, organ function, nutrition, and symptoms, and who had continuous intravenous inotropic support. All patients supported by extracorporeal membrane oxygenation (ECMO) were classified as INTERMACS level 1 and those supported by intraaortic balloon pumping without cardiogenic shock in order to maintain stable hemodynamics until LVAD implantation were classified as level 2. For the present study analysis, we divided all patients into 2 groups: INTERMACS level 1 (n=41) and level 2/3 (n=43). No patients in this study were classified as INTERMACS level 4 or higher. The study protocol was approved by the Institutional Review Board of the Osaka University Graduate School of Medicine. Individual patients were not identified in this study, thus individual consent was not required.

Devices

The details of device distribution are listed in Table 2. Most patients (56/84) underwent Nipro LVAD implantation because Nipro LVAD was the only commercially available device since the production of Novacor (WorldHeart Corp, Oakland, CA, USA) was terminated in 2006. Recently, clinical trials of new-generation LVADs such as the Jarvik 2000 (Jarvik Heart, Inc, New York, NY, USA), EVAHEART (Sun Medical Technology Research, Nagano, Japan), DuraHeart (Terumo Heart, Inc, Ann Arbor, MI, USA), and HeartMate II (Thoratec, Pleasanton, CA, USA) have been carried out in a limited group of patients without significant complications. DuraHeart, Jarvik 2000, and Heartware (HeartWare, Framingham, MA, USA) were also implanted in several patients at the Osaka University Hospital in a study supported by a Grant-in-Aid for scientific research from the Ministry of Health, Labor, and Welfare of the Japanese Government. The number of the different types of devices used is listed in Table 2. Patients who underwent Nipro LVAD implantation for bridge-to-bridge use, followed by a conversion to other continuous-flow LVADs were included with the Nipro LVAD recipient group. The majority of patients in the INTERMACS level 1 group underwent Nipro LVADs implantation. Implantable continuous-flow LVADs were more frequently used in the INTERMACS level 2/3 group because they were often used in clinical trials that excluded patients with cardiogenic shock.

All operative procedures were performed with either a median sternotomy or left thoracotomy, as previously described.[14]

Variables

Laboratory variables were adopted from laboratory data obtained just prior to LVAD implantation. In patients who required preoperative hemodiafiltration, the maximum preoperative Cr level was used for analysis. Renal function was assessed by calculating the glomerular filtration rate (GFR) using revised equations for estimated GFR (eGFR) from serum creatinine (Cr) for Japan, as follows (abbreviated): $GFR = 194 \times (Cr, mg/dl)^{-1.094} \times (age)^{-0.287} \times 0.739$ (if female).[15] The last echocardiographic parameters before LVAD implantation were used for left ventricular dimension (LVDd/Ds) and ejection fraction. Severe pulmonary congestion was defined as severely increasing bilateral pulmonary artery shadows and pulmonary edema involving the bilateral upper lobes.

Statistical Analysis

Continuous variables are expressed as mean±SD and were compared using the Student's t-test for unpaired data, where appropriate. Categorical variables were compared using Fisher's exact test. Univariate analysis was first applied using logistic regression for continuous variables and Fisher's exact test for categorical variables, and factors with $P<0.2$ were considered for a multivariate logistic model to identify the risk factor of 90-day mortality in the INTERMACS level 1 group. Kaplan-Meier analysis was used to estimate the overall survival rate. The survival rates were compared between the 2 groups using log-rank analysis, with a P value <0.05 considered significant. Cut-off values for serum Cr level and eGFR were calculated using a receiver operating characteristic (ROC) curve. Statistical analyses were performed using JMP 8.0 (SAS Institute, Cary, NC, USA).

Results

The preoperative patient demographics are summarized in Table 2. Approximately 70% of the patients were men with a median age of 38 years in the both groups. The leading etiology of heart failure was idiopathic dilated cardiomyopathy in both groups, but it was more frequent in the INTERMACS level 2/3 group. In contrast, almost all of the patients with acute myocardial infarction or fulminant myocarditis were included in the INTERMACS level 1 group. There was a certain device selection bias as previously mentioned. The number of patients who required preoperative mechanical support was much higher in the INTERMACS level 1 group. Preoperative laboratory data showed that the values of white

Table 2. Baseline Patient Characersistics

	Level 1 (n=41, %)	Level 2/3 (n=43, %)	P value
Age	38.9±2.4	38.4±2.4	0.899
Male	29/41 (70.7)	30/43 (69.8)	1.000
DCM	14 (34.1)	27 (62.8)	
ICM	3 (7.3)	5 (11.6)	
AMI	8 (19.5)	1 (2.3)	
Myocarditis	3 (7.3)	0 (0)	
dHCM	3 (7.3)	4 (9.3)	
Others	10 (24.4)	6 (14.0)	
Device	Nipro 35 (85.4), Jarvik2000 3 (7.3), HeartMateII 0 (0), EvaHeart 0 (0), DuraHeart 3 (7.3)	Nipro 23 (53.5), Jarvik2000 5 (11.6), HeartMateII 2 (4.7), EvaHeart 2 (4.7), DuraHeart 10 (23.3), HeartWare 1 (2.3)	0.002*
Implanbtable Continuous flow LVAD	6/41 (14.6)	20/43 (46.5)	0.002
IABP	32 (78.1)	12 (27.9)	<0.001
ECMO	28 (68.3)	0 (0)	<0.001
ECMO duration (days)	3.6±4.1		
Severe pulmonary congestion	18 (43.9)	6 (14.0)	0.003
Intubation	36 (87.8)	11 (25.6)	<0.001
CHDF	7 (17.1)	3 (7.0)	0.190
WBC ($10^3/\mu l$)	10.9±5.8	8.1±3.8	0.011
CRP (mg/dl)	7.8±7.8	3.1±5.6	0.002
AST (IU/dl)	414±1,080	164±665	0.209
ALT (IU/dl)	245±539	160±572	0.497
T-bil (mg/dl)	3.1±4.4	2.0±2.2	0.174
LDH (mg/dl)	1,253±1,998	443±799	0.021
BUN (mg/dl)	36.9±21.8	29.7±22.8	0.083
Cr (mg/dl)	1.63±0.98	1.43±1.14	0.400
eGFR (ml/min)	60.9±44.9	69.5±50.4	0.393
TP (mg/dl)	5.9±1.2	6.7±0.8	0.001
Alb (mg/dl)	2.9±0.5	3.5±0.6	<0.001
BNP (pg/μl)	1,334±880	788±595	0.006
LVDd (mm)	62.1±2.0	73.4±2.0	<0.001
LVDs (mm)	56.3±1.9	68.4±1.9	<0.001
EF (%)	19.1±1.5	19.9±1.5	0.696

DCM, idiopathic dilated cardiomyopathy; ICM, ischemic cardiomyopathy; AMI, acute myocardial infarction; dHCM, dilated phase hypertrophic cardiomyopathy; LVAD, left ventricular assist device; IABP, intraaortic balloon pumping; ECMO, extracorporeal membrane oxygenation; CHDF, continuous hemodiafiltration; WBC, white blood cell; CRP, C-reactive protein; AST, aspartate aminotransferase; ALT, alanine transaminase; T-bil, total bilirubin; LDH, lactate dehydrogenase; BUN, blood urea nitrogen; Cr, serum creatinine; eGFR, estimated calculated glomerular filtration rates; TP, serum total protein; Alb, serum albumin; BNP, brain natriuretic peptide; LVDd, left ventricular diastolic dimension; LVds, left ventricular systolic dimension; EF, LV ejection fraction.
*Fisher's exact test for Nipro LVAD and other devices.

blood cell counts and C-reactive protein were significantly higher in the INTERMACS level 1 group, and that the liver function and renal function were worse in this group but did not reach a statistically significant level. The serum total protein levels were significantly lower in the INTERMACS level 1 group, and their serum brain natriuretic peptide levels were significantly higher. A preoperative echocardiography showed more a dilated left ventricular dimension in the INTERMACS level 2/3 group patients. We compared the preoperative characteristics, early mortality, and cumulative survival rates between the 2 groups. To elucidate the preoperative risk factors for in-hospital death, which occurred most commonly within the first 90 days,[3] we performed a subset analysis of the INTERMACS level 1 group data to determine independent preoperative predictors for 90-day mortality.

The early results are shown in Table 3. The 90-day mortality was 24.4% (10/41) in the INTERMACS level 1 group. The causes of death in this group were multiple organ failure in 6 patients, cerebrovascular events in 3 patients, and sepsis in 1 patient. In the INTERMACS level 2/3 group, 1 patient died because of a cerebrovascular event within the first 90 days (P=0.003). To eliminate a device selection bias, we compared the early clinical results of Nipro LVAD implantation between the 2 groups. The 90-day mortality rate was also significantly higher in the INTERMACS level 1 group (28.6%) than in the INTERMACS level 2/3 group (4.4%) (P=0.037). The postoperative intubation period was significantly longer in the INTERMACS level 1 group (10.7 days) than in the INTERMACS level 2/3 group (2.4 days) (P=0.003). Postoperative continuous chronic hemodiafiltration (CHDF) was required in

Table 3. Early and Midterm Results of LVAD Implantation

	Level 1 (n=41)	Level 2/3 (n=43)	P value
30-day mortality in all patients	7 (17.1%)	0 (0%)	0.005
In Nipro LVAD patients	7/35 (20.0%)	0 /23 (0%)	0.035
Cause of death	MOF: 6, Cerebrovascular event: 1		
90-day mortality	10 (24.4%)	1 (2.3%)	0.003
In Nipro LVAD patients	10/35 (28.6%)	1/23 (4.4%)	0.037
Cause of death	MOF: 6, Sepsis:1, Cerebrovascular event: 3	Cerebrovascular event: 1	
Intubation period (days)	10.7±1.6	2.4±2.1	0.003
Postop CHDF	12 (29.3%)	3 (7.0%)	0.004
RVAD requirement	21 (51.2%)	2 (4.7%)	<0.001

MOF, multiple organ failure. Other abbreviations as in Table 2.

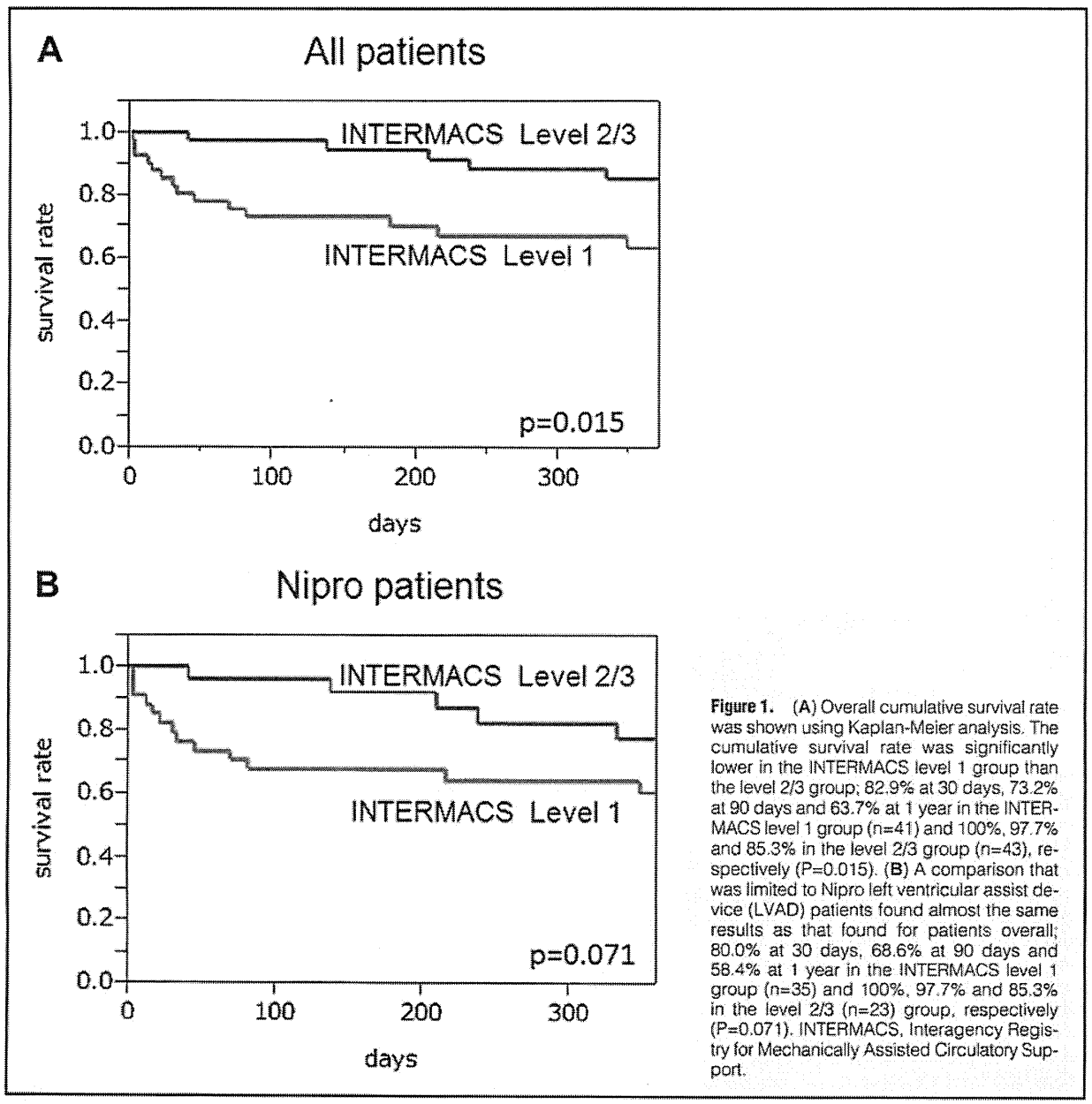

Figure 1. (A) Overall cumulative survival rate was shown using Kaplan-Meier analysis. The cumulative survival rate was significantly lower in the INTERMACS level 1 group than the level 2/3 group; 82.9% at 30 days, 73.2% at 90 days and 63.7% at 1 year in the INTERMACS level 1 group (n=41) and 100%, 97.7% and 85.3% in the level 2/3 group (n=43), respectively (P=0.015). (B) A comparison that was limited to Nipro left ventricular assist device (LVAD) patients found almost the same results as that found for patients overall; 80.0% at 30 days, 68.6% at 90 days and 58.4% at 1 year in the INTERMACS level 1 group (n=35) and 100%, 97.7% and 85.3% in the level 2/3 (n=23) group, respectively (P=0.071). INTERMACS, Interagency Registry for Mechanically Assisted Circulatory Support.

Table 4. Risk Factor of 90-Day Mortality in INTERMACS Level 1 Patients (n=41)

	Univariate		Multivariate	
	P value	OR (95%CI)	P value	OR (95%CI)
Age	0.571	1.01 (0.97–1.06)		
Male	0.231	4.95 (0.55–44.4)		
Nipro LVAD	0.307	*		
Severe pulmonary congestion	0.264	2.27 (0.50–10.25)		
IABP	1.000	1.17 (0.20–6.80)		
ECMO	0.458	2.20 (0.40–12.2)		
CHDF	<0.001	45.0 (4.25–476.6)	**	
Cr (mg/dl)	0.003	6.41 (2.24–28.4)	0.003	8.51 (1.86–109.3)
T-bil (mg/dl)	0.499	1.05 (0.89–1.23)		
CRP (mg/dl)	0.213	1.06 (0.97–1.17)		
TP (mg/dl)	0.100	0.56 (0.26–1.07)	0.155	0.46 (0.11–1.33)
BNP (pg/ml)	0.246	1.00 (0.99–1.00)		

Abbreviations as in Tables 1,2.
*OR of Nipro LVAD are not available due to complete separation. **CHDF was not entered into the multivariate analysis.

12 (29.3%) patients in the INTERMACS level 1 group and 3 (7.0%) patients in the INTERMACS level 2/3 group (P=0.004). Almost half of the patients (21/41) in the INTERMACS level 1 group needed RVAD for temporary right heart support, and 9 of them required long-term RVAD support, for which Nipro or Jarvik 2000 were used.[16]

The majority of in-hospital deaths in both groups occurred within the first 3 months, as shown by the cumulative survival rates presented in **Figure 1**. Overall cumulative survival rates are shown in **Figure 1A**. Cumulative survival rates were significantly lower in the INTERMACS level 1 group (82.9% at 30 days, 75.6% at 90 days, and 63.7% at 1 year) than in the INTERMACS level 2/3 group, (100% at 30 days, 97.7% at 90 days, and 85.3% at 1 year) (P=0.015). To eliminate a device selection bias, we evaluated cumulative survival rates in Nipro LVAD-implanted patients; **Figure 1B** shows the cumulative survival rates in these groups of patients, which were 80.0% at 30 days, 71.4% at 90 days, and 58.4% at 1 year in the INTERMACS level 1 group, and 100% at 30 days, 95.6% at 90 days, and 73.8% at 1 year in level 2/3 group (P=0.071). As shown in **Figures 1A** and **B**, the majority of deaths in the INTERMACS level 1 group occurred within the first 3 months, which was significantly different to that of the INTERMACS level 2/3 group, although there was no statistically significant difference in regard to NIPRO patients. In contrast, the rates of mortality were quite similar between the 2 groups from 3 months after LVAD implantation.

Because there are still many INTERMACS level 1 patients who undergo LVAD implantation in Japan, we performed a subset analysis for the patients within this group. The results of the univariate and multivariate analyses of the risk factors for 90-day mortality rates in the INTERMACS level 1 group are shown in **Table 4**. The multivariate analysis identified preoperative serum Cr level as an independent predictor of 90-day mortality. Although the requirement of RVAD was found to be a significant risk factor for long-term mortality in our previous study, we did not include RVAD requirement as a factor in this subset multivariate analysis because we evaluated 'preoperative' risk factors for 90-day mortality.[14]

ROC curve results showed that a preoperative level of Cr of 1.96 mg/dl was an optimal cut-off value for 90-day mortality, with a sensitivity of 80.0% and specificity of 81.7%, while a preoperative eGFR level of 25.0 ml/min had a sensitivity of 70.0% and specificity of 77.4% (**Figures 2A–C**). **Figure 3** shows the cumulative survival rates of patients with or without preoperative serum Cr level of >1.96 mg/dl. The actual survival rates were 96.2% at 30 days, 88.0% at 90 days, and 77.5% at 1 year in patients with Cr levels of <1.96 mg/dl, and 60.0% at 30 days, 46.7% at 90 days, and 31.1% at 1 year in patients with Cr levels of ≥1.96 mg/dl (P=0.0011).

Contrary to previous reports, our results showed that the preoperative requirement of ECMO was not an independent risk factor of mortality.[17] Therefore, we performed a subset analysis for the patients within the INTERMACS level 1 group treated with or without preoperative ECMO support. **Figure 4** shows the cumulative survival rates of patients in the INTERMACS level 1 group categorized according to renal function level and preoperative ECMO requirement. Regardless of the preoperative ECMO support, patients with serum Cr levels of <1.96 mg/dl had a better prognosis than patients with serum Cr levels of >1.96 mg/dl (P=0.018).

Discussion

In our previous study published in 2010, we concluded that age at implantation and requirement of RVAD were significant risk factors for long-term mortality of patients undergoing LVAD implantation.[14] However, it is important to distinguish long-term mortality from perioperative mortality, because the cause of death varies depending on the period. Hence, in the present study, we evaluated preoperative factors related to early mortality to elucidate the optimal timing for LVAD implantation for patients with severe heart failure.

In the second INTERMACS annual report, it was found that LVAD implantation in INTERMACS level 2/3 patients led to a better prognosis than that of INTERMACS level 1 patients.[12] Our results are consistent with those results. Although a paracorporeal pulsatile device was more frequently used in our study, the cumulative survival rates following device implantation were similar to those reported in the second INTERMACS annual report.[12] Lietz et al reported that the majority (79%) of in-hospital deaths occurred during the first 3 months of LVAD implantation,[3] and our results confirm these data. As shown in **Figure 1**, most deaths occurred within the first 3 months and contributed to the significant difference between the 2 groups, whereas the survival rate after 3 months was

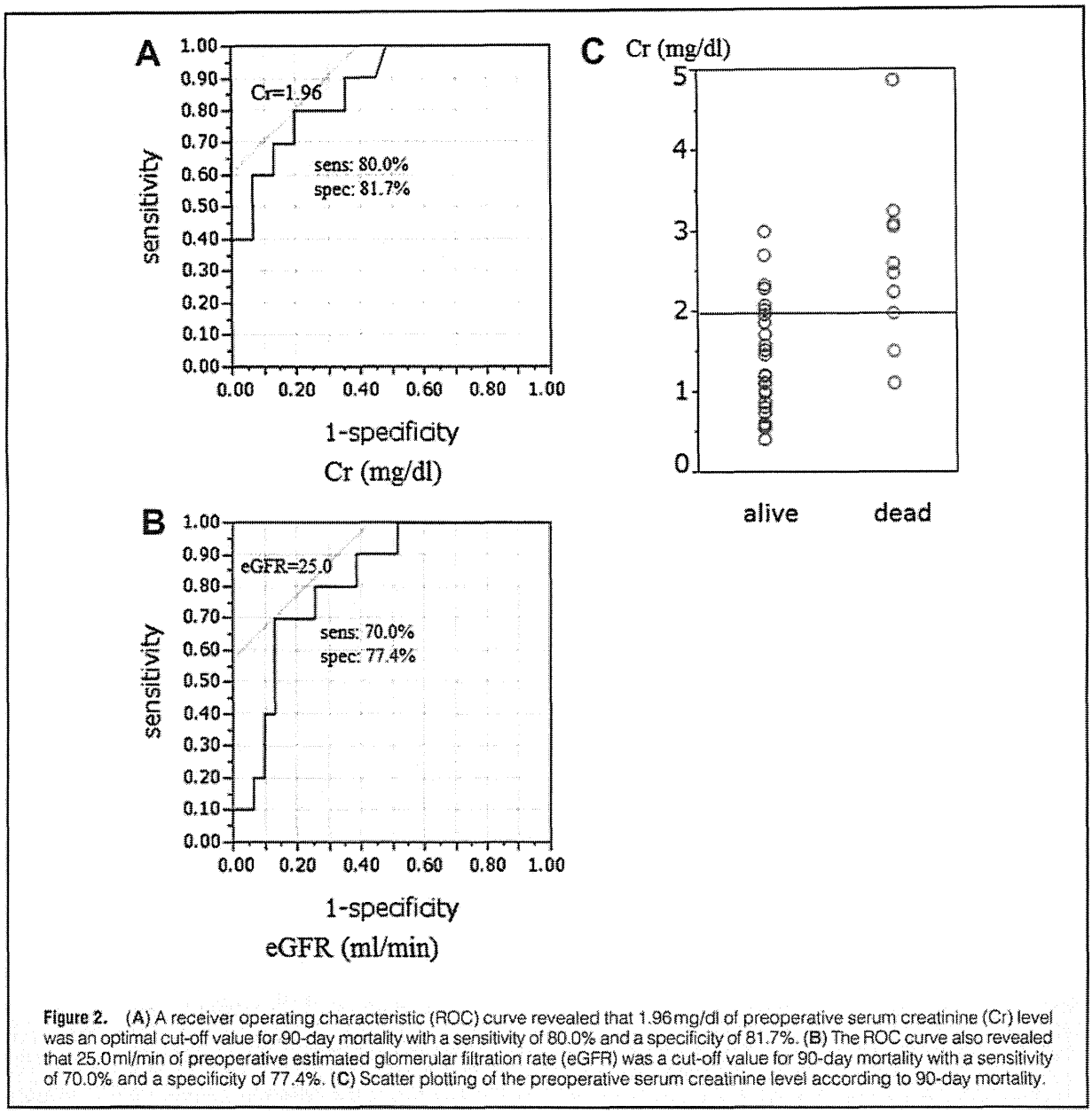

Figure 2. (A) A receiver operating characteristic (ROC) curve revealed that 1.96 mg/dl of preoperative serum creatinine (Cr) level was an optimal cut-off value for 90-day mortality with a sensitivity of 80.0% and a specificity of 81.7%. (B) The ROC curve also revealed that 25.0 ml/min of preoperative estimated glomerular filtration rate (eGFR) was a cut-off value for 90-day mortality with a sensitivity of 70.0% and a specificity of 77.4%. (C) Scatter plotting of the preoperative serum creatinine level according to 90-day mortality.

similar between the groups. Following elimination of device selection bias, analysis of patients with a Nipro LVAD implant showed nearly the same results as that found with all of the patients, with no significant difference. These results suggest that early mortality depends more on preoperative status than the type of device used. In support of this, we observed that the most frequent cause of early death was multi-organ failure, which was often already present preoperatively, rather than device-related complications such as drive-line infection and cerebrovascular events. In contrast, preoperative INTERMACS classification seems to have no relationship to long-term mortality from 3 months after implantation.

The post-LVAD comorbidities were significantly more frequent in patients in the INTERMACS level 1 group (**Table 3**). Patients in the INTERMACS level 1 group more often required prolonged mechanical ventilation and postoperative continuous hemodialysis. Previous studies including our study showed that RVAD requirement was a significant predictor of overall mortality and device-related infections.[14,18,19] In more recent studies, it was reported that laboratory variables, which are indirectly related to RV function (eg, bilirubin and Cr levels), were more strongly associated with the need for biventricular support than with the preoperative hemodynamic variables.[19,20] Therefore, early LVAD implantation before a progressive decline of end-organ function is essential to prevent these postoperative complications.

Nonetheless, there are still many patients in INTERMACS level 1 group with progressive end-organ dysfunction referred to us for LVAD implantation. Thus, we performed a subset risk analysis for early mortality for INTERMACS level 1 patients (**Table 4**).

Univariate and multivariate analysis for the INTERMACS

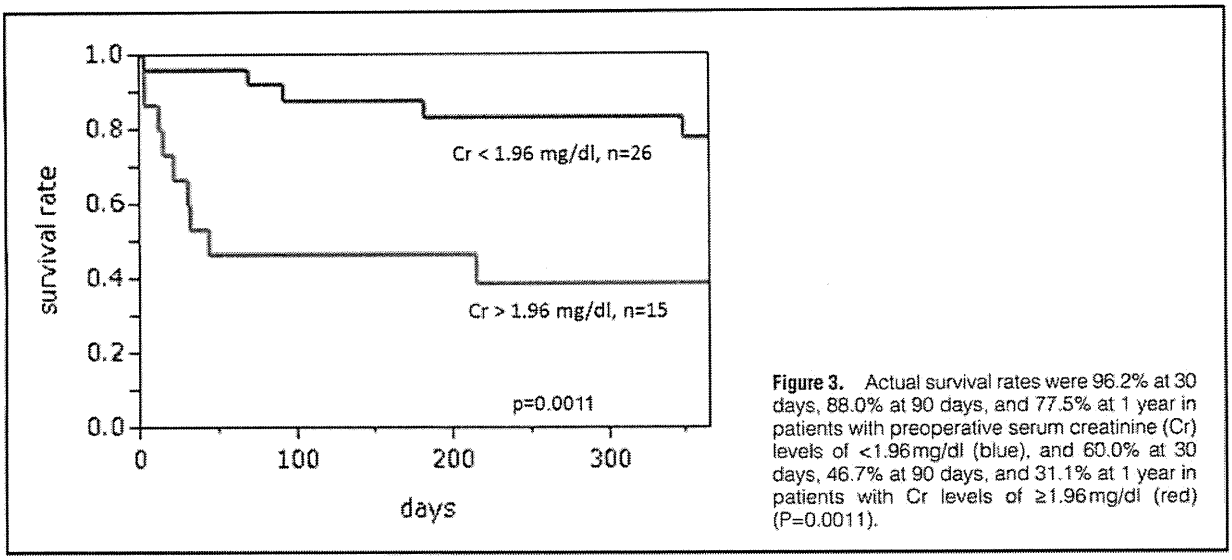

Figure 3. Actual survival rates were 96.2% at 30 days, 88.0% at 90 days, and 77.5% at 1 year in patients with preoperative serum creatinine (Cr) levels of <1.96 mg/dl (blue), and 60.0% at 30 days, 46.7% at 90 days, and 31.1% at 1 year in patients with Cr levels of ≥1.96 mg/dl (red) (P=0.0011).

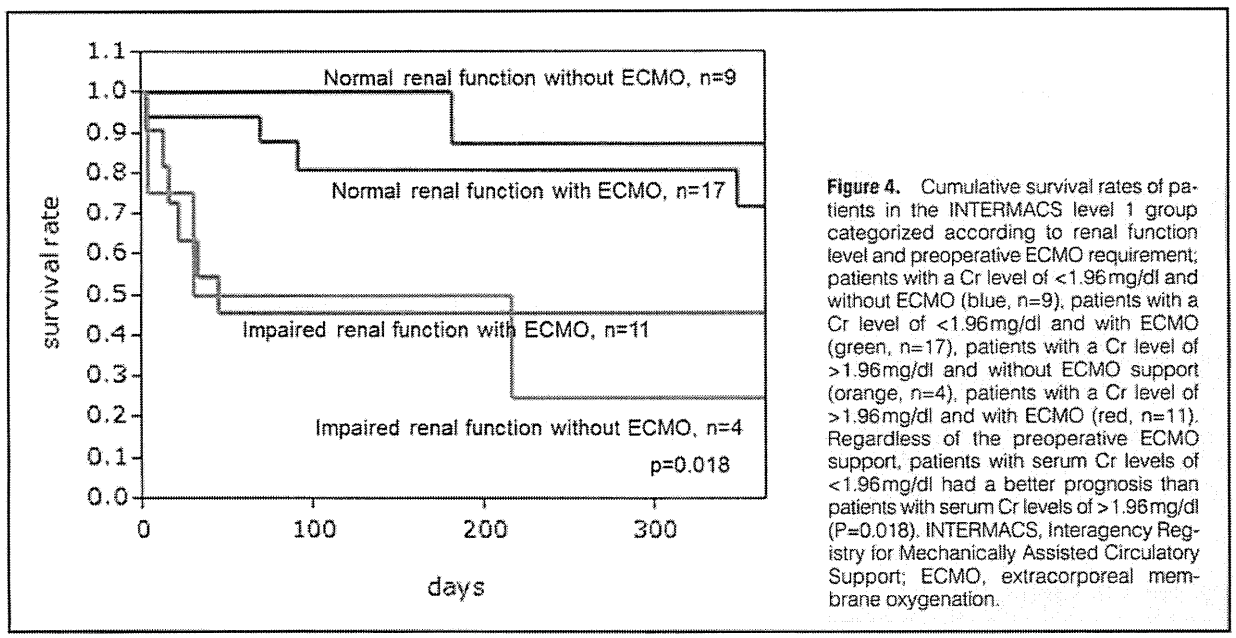

Figure 4. Cumulative survival rates of patients in the INTERMACS level 1 group categorized according to renal function level and preoperative ECMO requirement; patients with a Cr level of <1.96 mg/dl and without ECMO (blue, n=9), patients with a Cr level of <1.96 mg/dl and with ECMO (green, n=17), patients with a Cr level of >1.96 mg/dl and without ECMO support (orange, n=4), patients with a Cr level of >1.96 mg/dl and with ECMO (red, n=11). Regardless of the preoperative ECMO support, patients with serum Cr levels of <1.96 mg/dl had a better prognosis than patients with serum Cr levels of >1.96 mg/dl (P=0.018). INTERMACS, Interagency Registry for Mechanically Assisted Circulatory Support; ECMO, extracorporeal membrane oxygenation.

level 1 patients showed pre-existing renal dysfunction as the independent risk factor for early mortality. A ROC curve (Figure 2) showed that a preoperative Cr level of 1.96 mg/dl was an optimal cut-off value for early mortality, and patients without severe renal impairment (Cr level <1.96 mg/dl) showed significantly better prognosis than patients with impaired renal function (Cr ≥1.96 mg/dl) (Figure 3). Sandner et al found that the survival rates of patients whose GFR was <60 ml·min^{-1}·1.73 m^{-2} at LVAD implantation were significantly worse than those of patients with GFR >60 ml·min^{-1}·1.73 m^{-2}.[21] In addition, Butler et al reported that patients with Cr clearance (CrCl) values of <47 ml/min had a significantly higher risk of mortality than patients with CrCl values of >95 ml/min (OR: 1.95; 95%CI, 1.14–3.63).[22] Although preoperative renal dysfunction sometimes improves after LVAD implantation, those patients often require perioperative CHDF after LVAD implantations, resulting in prolonged ICU stay and increased risks of other complications such as catheter infection and prolonged mechanical ventilations, and therefore might increase early mortality. These results suggests that LVAD implantation should be considered without delay for patients with end-stage heart failure if renal function progressively declines despite optimal medical therapy.

In the present study, the preoperative serum bilirubin level was not found to be the independent risk factor for 90-day mortality in logistic regression analysis. In addition, our previous study using a Cox-hazard model also revealed that serum bilirubin was not the independent risk factor for long-term mortality.[14] These results do not agree with those of several previous studies.[1,20,23] The reason for this discrepancy might be that we aggressively implant a temporary RVAD at the time of LVAD implantation if the patient is regarded as high risk for insufficient hemodynamic with exclusive LVAD support. Fitzpatrick et al recommended proceeding directly to

biventricular assist device implantation in patients at high risk for failure of isolated LVAD support, because early institution of biventricular support results in a dramatic improvement in survival.[24] In the present study, approximately half of our patients in the INTERMACS level 1 group underwent simultaneous RVAD implantation, of whom 6 of 21 were weaned from temporary RVAD support.

Interestingly, preoperative mechanical support with ECMO was not a significant risk factor for early death in our study, whereas Klotz et al reported that preoperative ECMO support was one of the independent risk factors of ICU mortality.[17] As shown in Figure 4, the cumulative survival curve mainly depends on the existence of renal dysfunction rather than on ECMO support. According to Lietz et al, the risk of LVAD surgery was not correlated with the hemodynamic severity of heart failure but was correlated with the presence of comorbidities.[3] We believe that mechanical support itself is useful to prevent end-organ dysfunction. We now believe that immediate ECMO support should be provided for patients with progressively declining renal function due to refractory heart failure, and LVAD implantation should be considered without delay if further deterioration of end-organ function is noted even with ECMO support.

Study Limitation

There are several limitations in the present study. First, the main limitation is that our study was a retrospective study limited to a single institution. There was a device selection bias between INTERMACS level 1 and level 2/3 groups because of the use of new continuous-flow devices in clinical trials. Preoperative hemodynamic variables such as right ventricular stroke work (RVSW) and the RVSW index could not be obtained in more than 25% of the patients and was not considered while calculating the results. We did not distinguish between acute renal failure and chronic renal failure, which is more refractory to LVAD implantation. In addition, in patients with preoperative hemodiafiltration, the serum Cr level did not indicate precise renal function. Another limitation is the fact that the differences of LVAD performance due to the use of different devices, which might influence systemic circulation and mortality, were not evaluated.

Conclusions

Our data show that LVAD implantation in stable conditions contributes to a better clinical outcome for patients with severe heart failure. If critical cardiogenic shock occurs, LVAD implantation must be considered immediately before any impairment of other end-organ functions, especially renal function.

Disclosures

Conflict of interest: None.

References

1. Frazier OH, Rose EA, Oz MC, Dembitsky W, McCarthy P, Radovancevic B, et al. Multicenter clinical evaluation of the HeartMate vented electric left ventricular assist structure in patients awaiting heart transplantation. *J Thorac Cardiovasc Surg* 2001; **122:** 1186–1195.
2. Rose EA, Gelijns AC, Moskowitz AJ, Heitjan DF, Stevenson LW, Dembitsky W, et al. Long-term use of a left ventricular assist device for end-stage heart failure. *N Eng J Med* 2001; **345:** 1435–1443.
3. Lietz K, Long JW, Kfoury AG, Slaughter MS, Silver MA, Milano CA, et al. Outcomes of left ventricular assist device implantation as destination therapy in the post-REMATCH era: Implications for patient selection. *Circulation* 2007; **116:** 497–505.
4. Miller LW, Pagani FD, Russell SD, John R, Boyle AJ, Aaronson KD, et al. Use of a continuous-flow device in patients awaiting heart transplantation. *N Eng J Med* 2007; **357:** 885–896.
5. Rogers JG, Aaronson KD, Boyle AJ, Russell SD, Milano CA, Pagani FD, et al; HeartMate II Investigators. Continuous flow left ventricular assist device improves functional capacity and quality of life of advanced heart failure patients. *J Am Coll Cardiol* 2010; **55:** 1826–1834.
6. Pagani FD, Miller LW, Russell SD, Aaronson KD, John R, Boyle AJ, et al; HeartMate II Investigators. Extended mechanical circulatory support with a continuous-flow rotary left ventricular assist device. *J Am Coll Cardiol* 2009; **54:** 312–321.
7. Slaughter MS, Rogers JG, Milano CA, Russell SD, Conte JV, Feldman D, et al; HeartMate II Investigators. Advanced heart failure treated with continuous-flow left ventricular assist device. *N Engl J Med* 2009; **361:** 2241–2251.
8. Kamdar F, Boyle A, Liao K, Colvin-adams M, Joyce L, John R. Effects of centrifugal, axial, and pulsatile left ventricular assist device support on end-organ function in heart failure patients. *J Heart Lung Transplant* 2009; **28:** 352–359.
9. Radovancevic B, Vrtovec B, de Kort E, Radovancevic R, Gregoric ID, Frazier OH. End-organ function in patients on long-term circulatory support with continuous- or pulsatile-flow assist devices. *J Heart Lung Transplant* 2007; **26:** 815–818.
10. Stevenson LW, Pagani FD, Young JB, Jessup M, Miller L, Kormos RL, et al. INTERMACS profiles of advanced heart failure: The current picture. *J Heart Lung Transplant* 2009; **28:** 535–541.
11. Kirklin JK, Naftel DC, Stevenson LW, Kormos RL, Pagani FD, Miller MA, et al. INTERMACS database for durable devices for circulatory support: First annual report. *J Heart Lung Transplant* 2008; **27:** 1065–1072.
12. Kirklin JK, Naftel DC, Kormos RL, Stevenson LW, Pagani FD, Miller MA, et al. Second INTERMACS annual report: More than 1,000 primary left ventricular assist device implants. *J Heart Lung Transplant* 2010; **29:** 1–10.
13. Kamata S, Sakaguchi T, Miyagawa S, Yoshikawa Y, Yamauchi T, Takeda K, et al. The first clinical case in Japan of destination therapy using the Jarvik 2000 left ventricular assist device. *J Artif Organs* 2010; **13:** 170–173.
14. Saito S, Matsumiya G, Sakaguchi T, Miyagawa S, Yoshikawa Y, Yamauchi T, et al. Risk factor analysis of long-term support with left ventricular assist system. *Circ J* 2010; **74:** 715–722.
15. Matsuo S, Imai E, Horio M, Yasuda Y, Tomita K, Nitta K, et al. Revised equations for estimated GFR from serum creatinine in Japan. *Am J Kidney Dis* 2009; **53:** 982–992.
16. Saito S, Sakaguchi T, Miyagawa S, Yoshikawa Y, Yamauchi T, Ueno T, et al. Biventricular support using implantable continuous-flow ventricular assist devices. *J Heart Lung Transplant* 2011; **30:** 475–478.
17. Klotz S, Vahlhaus C, Riehl C, Reitz C, Sindermann JR, Scheld HH. Pre-operative prediction of post-VAD implant mortality using easily accessible clinical parameters. *J Heart Lung Transplant* 2010; **29:** 45–52.
18. Kormos RL, Teuteberg JJ, Pagani FD, Russell SD, John R, Miller LW, et al. Right ventricular failure in patients with the HeartMate II continuous-flow left ventricular assist device: Incidence, risk factors, and effect on outcomes. *J Thorac Cardiovasc Surg* 2010; **139:** 1316–1324.
19. Farrar DJ, Hill JD, Pennington DG, McBride LR, Holman WL, Kormos RL, et al. Preoperative and postoperative comparison of patients with univentricular and biventricular support with the Thoratec ventricular assist device as a bridge to cardiac transplantation. *J Thorac Cardiovasc Surg* 1997; **113:** 202–209.
20. Matthews JC, Koelling TM, Pagani FD, Aaronson KD. The right ventricular failure risk score a pre-operative tool for assessing the risk of right ventricular failure in left ventricular assist device candidates. *J Am Coll Cardiol* 2008; **51:** 2163–2172.
21. Sandner SE, Zimpfer D, Zrunek P, Rajek A, Schima H, Dunkler D, et al. Renal function and outcome after continuous flow left ventricular assist device implantation. *Ann Thorac Surg* 2009; **87:** 1072–1078.
22. Butler J, Geisberg C, Howser R, Portner PM, Rogers JG, Deng MC, et al. Relationship between renal function and left ventricular assist device use. *Ann Thorac Surg* 2006; **81:** 1745–1751.
23. Shiga T, Kinugawa K, Hatano M, Yao A, Nishimura T, Endo M, et al. Age and preoperative total bilirubin level can stratify prognosis after extracorporeal pulsatile left ventricular assist device implantation. *Circ J* 2010; **75:** 121–128.
24. Fitzpatrick JR 3rd, Frederick JR, Hiesinger W, Hsu VM, McCormick RC, Kozin ED, et al. Early planned institution of biventricular mechanical circulatory support results in improved outcomes compared with delayed conversion of a left ventricular assist device to a biventricular assist device. *J Thorac Cardiovasc Surg* 2009; **137:** 971–977.

Circulation Journal
Official Journal of the Japanese Circulation Society
http://www.j-circ.or.jp

RAPID COMMUNICATION

First Pediatric Heart Transplantation From a Pediatric Donor Heart in Japan

Takayoshi Ueno, MD, PhD; Norihide Fukushima, MD, PhD; Taichi Sakaguchi, MD, PhD; Haruki Ide, MD; Hideto Ozawa, MD; Shunsuke Saito, MD; Hajime Ichikawa, MD, PhD; Yoshiki Sawa, MD, PhD

Background: Since the revision of the Japanese Organ Transplantation Act, children younger than 15 years old can donate their organs after brain death.

Methods and Results: A teenage boy with endstage restrictive cardiomyopathy underwent the first heart transplantation with a pediatric donor heart in Japan on April 12, 2011. He had a good postoperative clinical course and no histological rejection episodes. His waiting period was relatively short (237 days) compared with adult patients, because of the pediatric patient-first policy for a pediatric donor heart.

Conclusions: To increase pediatric heart transplantation in Japan, further enlightenment of the general population about pediatric organ donation is desirable. (*Circ J* 2012; **76:** 752–754)

Key Words: Cardiomyopathy; Pediatrics; Transplantation

Orthotropic heart transplantation (HTx) has been gradually increasing in Japan since the first HTx was performed in Osaka University Hospital in February 1999. However, because of the long waiting period for HTx, long-term support of that patient with ventricular support system was needed.[1] Until continuous flow assist devices could be approved, and the postoperative prognosis thus improved,[2] the results of HTx would be unsatisfactory. Moreover, children under the age of 15 years could not donate their organs after brain death until the Japanese Organ Transplantation Act was revised on 17 July, 2010, because in Japan only persons who had given written consent for organ donation after brain death could donate their organs. Prior to the case reported here, only 4 teenage HTx had been performed, using adult donor hearts.

After renewal of the Act, organs can be donated after brain death by consent of the patient's relatives, if he or she did not deny organ donation, allowing children younger than 15 years of age to donate.

Before issuing the revised Act, new guidelines for organ allocation were made and because of the beneficial effects of pediatric donor hearts on survival after pediatric HTx, the pediatric patient-first policy from a pediatric donor heart was made the same as the policy of the United Network for Organ Sharing. Briefly, within each heart status, a heart retrieved from a pediatric organ donor less than 18 years of age shall be allocated to a pediatric heart candidate (ie, less than 18 years old at the time of listing) before the heart is allocated to an adult candidate.

We report the first pediatric HTx with a heart from a donor under 15 years of age in Japan.

A teenage boy was admitted to Osaka University Hospital on April 12th 2011 by helicopter transportation from his local hospital. In April 2007, he fainted for the first time in his life, because of complete atrioventricular block. He underwent VDD mode pacemaker implant at his local hospital. Histological examination of the right ventricular myocardium revealed chronic myocarditis. Because there was progressive worsening of his clinical condition over the next few years, implantation of a pacemaker for cardiac resynchronized therapy was attempted, but it failed because another pacemaker lead could not be placed in a suitable site in the coronary sinus.

In July 2009, he was admitted for acute renal failure accompanied by dehydration and diarrhea. Since then, he repeatedly showed digestive symptoms of heart failure and was admitted to his local hospital. The highest level of B-type natriuretic peptide was 4,200 pg/ml. In April 2010, continuous dopamine administration at a dose of $3\,\mu g \cdot kg^{-1} \cdot min^{-1}$ was started, but despite inotropic support he was diagnosed by cardiac catheterization as having restrictive cardiomyopathy with left ventricular systolic dysfunction. In August 2010, he was listed for HTx because of advanced restricted cardiomyopathy. He was waiting for HTx at his local hospital.

On April 12th 2011, the donor information was brought to Osaka University Hospital: the donor was between 10 and 15

Received October 6, 2011; revised manuscript received January 15, 2012; accepted January 16, 2012; released online January 25, 2012 Time for primary review: 39 days

Department of Cardiovascular Surgery, Osaka University Graduate School of Medicine, Suita (T.U., N.F., T.S., H. Ide, H.O., S.S., Y.S.); Department of Pediatric Cardiovascular Surgery, National Cerebral and Cardiovascular Center, Suita (H. Ichikawa), Japan

Mailing address: Takayoshi Ueno, MD, PhD, Department of Cardiovascular Surgery, Osaka University Graduate School of Medicene, 1-7 Yamadaoka, Suita 565-0871, Japan. E-mail: uenotm@surg1.med.osaka-u.ac.jp

ISSN-1346-9843 doi:10.1253/circj.CJ-11-1001

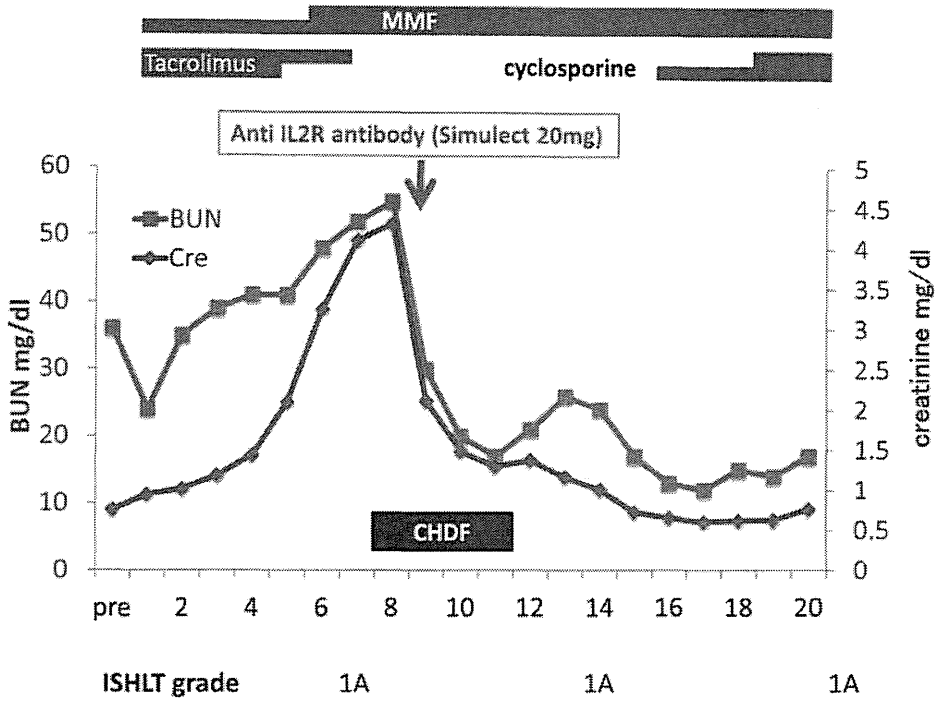

Figure. Creatinine, blood urea nitrogen (BUN) levels before and post transplantation, and postoperative immunosuppressive regimen. Cre, creatinine; MMF, mycophenolate mofetil; CHDF, continuous hemodiafiltration.

years old, the donor heart's function was good for transplantation (EF 69%), and the weight ratio of the donor and the recipient was –5%. The next day, HTx was performed with the bicaval method. The total ischemic time was 220 min. The waiting period for HTx had been 237 days.

The immediate postoperative course was good and he was extubated on postoperative day (POD) 1; 3 doses of methylprednisolone (125 mg) were given intravenously on the day of operation and POD 1 on each day. A triple oral immunosuppression regimen with tacrolimus, mycophenolate mofetil and prednisolone was started on POD 1. The tacrolimus target trough level was 10–15 ng/ml for the first week after HTx. No induction therapy was used. From POD 4, the serum creatinine level and his weight gradually increased, and on POD 8 the patient required continuous hemodiafiltration (CHDF) and mechanical respiratory support because of progressive dyspnea (Figure). Tacrolimus was discontinued because of its nephrotoxity, and a chimeric monoclonal antibody against the interleukin-2 receptor α-chain, basiliximab, at a dose of 20 mg was given intravenously on POD 9 to spare the use of calcineurin inhibitors (CNI) during recovery of renal function. After the serum creatinine level decreased to 1 mg/dl, mechanical ventilation was discontinued on POD 11 and CHDF on POD 12. Oral administration of cyclosporine instead of tacrolimus was started, at a low initial dose, on POD 16, and the dose was gradually increased to give a blood trough level of approximately 250 mg/ml. After rehabilitation, the patient was discharged in good clinical condition on POD 50. Echocardiographic examination showed excellent biventricular EF. There were no clinical or histological episodes of rejection during the postoperative course. The serum creatinine level was 0.8 mg/dl at discharge.

Discussion

In Japan, HTx has increased since the revised Organ Transplant Act enforcement in July 2010; 34 HTx were performed in the 10 months after the revision of the Act, whereas only 69 had been done in the nearly 13 years after the old Act was first issued. Of the 103 HTx performed in Japan, only 5 patients have died after HTx and the 10-year survival after HTx is more than 95%, which is much better than the outcomes from the data of the International Society for Heart and Lung (ISHLT) Registry.

Only a limited number of teenage pediatric HTx were performed in Japan, because children younger than 15 years old could not donate their organs after brain death under the old Organ Transplant Act. Worldwide, since the ISHLT registry was started in 1982, the number of pediatric HTx has gradually increased.[3] In recent years, the number has remained stable at approximately 450 per year, and a total of 8,575 pediatric HTx was reported before 2008. Overall survival was approximately 40% for patients up to 20 years after transplantation. The median survival was 18.3 years for infant recipients, 15.5 years for childhood-age recipients, and 11.3 years for adolescents. Moreover, HTx outcomes have improved era by era, even in sicker children who may have been excluded previously.[4,5] It is certain that HTx is the major treatment for severe heart failure, even in the pediatric population.

When cyclosporine is the primary CNI, a significantly greater percentage of patients are treated for rejection than occurs with tacrolimus. Patients receiving cyclosporine at discharge have a 45% incidence of rejection in the first year compared with 27% for those discharged with tacrolimus therapy, ac-

cording to the ISHLT Registry.[3] Therefore, we chose a triple immunosuppressive regimen based on tacrolimus. In Japan, no drugs for induction therapy after HTx are approved for use by the Government, so no induction was done initially. Because CHDF and mechanical ventilation were required in the present case, because of acute renal failure, tacrolimus was discontinued and anti-IL2R antibody was used to reduce the use of CNIs. After renal function was restored, we switched to cyclosporine. CNIs are still the basis of immunosuppressive therapy in HTx, but there are numerous side effects, such as renal failure, hypertension, hyperlipidemia, etc.[6] Acute nephrotoxicity occurs soon after the onset of administration of CNIs, and the nephrotoxity is dose-dependent and characterized by acute vasoconstriction of kidney arterioles and arteries.[7] Additionally, renal dysfunction is frequently seen under the condition of pretransplant heart failure.[8] The present patient had mild renal dysfunction prior to HTx, because of the high central venous pressure (25 mmHg) caused by the restrictive cardiomyopathy. As his reserve capacity of renal function may have been decreased during the posttranplant period, CNIs caused additional deterioration in renal function, and CHDF was required as a result. In the case of deteriorated renal reserve capacity before HTx, other immunosuppressive regimens such as induction therapy and/or mammalian target of rapamycin inhibitors (mTORi) might be recommended. Primary induction therapy using an IL2R-antagonist, which is not approved for use in Japan after HTx, might be better for avoiding renal insufficiency. The trend for induction therapy with polyclonal antilymphocyte/antithymocyte globulin or IL2R-antagonist has increased recently, with more than 70% receiving it in 2009.[3] These medicines for induction therapy should be covered by insurance for HTx in Japan as soon as possible. On the other hand, CNI-free immunosuppression after cardiac transplantation using MMF and the mTORi, sirolimus, showed a good clinical course in the absence of acute rejection in a patient with impaired renal function.[9] In Japan, the mTORi, everolimus, is already approved for use after HTx. However, as mTORi have several side effects, such as impairment of wound healing, hypercholesterolemia, inhibition of sperm production and so on, we did not chose everolimus as the first choice after pediatric HTx.

On issuing the revised Act, the pediatric patient-first policy from a pediatric donor heart was made the same as the policy of the United Network for Organ Sharing. Therefore, the patient waited only 237 days for HTx, whereas the recent average waiting period for an adult donor heart with the same blood type was 1,008 days.

In conclusion, we successfully performed the first pediatric HTx from a pediatric donor heart under the pediatric patient-first policy in Japan. However, most pediatric patients requiring HTx die within a year while waiting. To increase pediatric HTx in Japan, further enlightenment of pediatric organ donation, establishment of pediatric emergency systems, intensive care systems, and pediatric mechanical circulatory support systems are needed. We desire that a pediatric HTx will soon be carried out in a young child, especially one who is less than 10 years old.

References

1. Saito S, Matsumiya G, Sakaguchi T, Miyagawa S, Yoshikawa Y, Yamauchi T, et al. Risk factor analysis of long-term support with left ventricular assist system. *Circ J* 2010; **74:** 715–722.
2. Kinugawa K. How to treat stage D heart failure? When to implant left ventricular assist devices in the era of continuous flow pumps? *Circ J* 2010; **74:** 233–239.
3. Kirk R, Edwards LB, Kucheryavaya AY, Aurora P, Christie JD, Dobbels F, et al. Registry of the international society for heart and lung transplantation: Thirteenth official pediatric heart transplantation report 2010. *J Heart Lung Transplant* 2010; **29:** 1119–1128.
4. Singh TP, Edwards LB, Kirk R, Boucek MM. Era effect on post-transplant survival adjusted for baseline risk factors in pediatric heart transplant recipients. *J Heart Lung Transplant* 2009; **28:** 1285–1291.
5. Irving CA, Kirk R, Parry G, Hamilton L, Dark JH, Wrightson N, et al. Outcomes following more than two decades of paediatric cardiac transplantation. *Eur J Cardiothorac Surg* 2011; **40:** 1197–1202.
6. Hertz MI, Aurora P, Boucek MM, Christie JD, Dobbels F, Edwards LB, et al. Registry of the International Society for Heart and Lung Transplantation: Introduction to the 2007 annual reports–100,000 transplants and going strong. *J Heart Lung Transplant* 2007; **26:** 763–768.
7. Tönshoff B, Höcker B. Treatment strategies in pediatric solid organ transplant recipients with calcineurin inhibitor-induced nephrotoxicity. *Pediatr Transplant* 2006; **10:** 721–729.
8. Shlipak M, Massie B. The clinical challenge of cardiorenal syndrome. *Circulation* 2004; **110:** 1514–1517.
9. Groetzner J, Kaczmarek I, Schulz U, Stegemann E, Kaiser K, Wittwer T, et al; VENINAHTx-Investigator. Mycophenolate and sirolimus as calcineurin inhibitor-free immunosuppression improves renal function better than calcineurin inhibitor-reduction in late cardiac transplant recipients with chronic renal failure. *Transplantation* 2009; **87:** 726–733.

Circulation Journal
Official Journal of the Japanese Circulation Society
http://www.j-circ.or.jp

ORIGINAL ARTICLE
Cardiovascular Surgery

Initial Experience of Conversion of Toyobo Paracorporeal Left Ventricular Assist Device to DuraHeart Left Ventricular Assist Device

Daisuke Yoshioka, MD; Taichi Sakaguchi, MD, PhD; Shunsuke Saito, MD; Shigeru Miyagawa, MD, PhD; Hiroyuki Nishi, MD; Yasushi Yoshikawa, MD; Satsuki Fukushima, MD, PhD; Takayoshi Ueno, MD, PhD; Toru Kuratani, MD, PhD; Yoshiki Sawa, MD, PhD

Background: This report details experience of the conversion of the Toyobo left ventricular assist device (LVAD; Nipro, Osaka, Japan) to the DuraHeart LVAD (TerumoHeart, Ann Arbor, MI, USA) in patients awaiting heart transplantation.

Methods and Results: Eight patients (4 male, 4 female) with Toyobo paracorporeal LVAD underwent conversion to the third-generation centrifugal (DuraHeart) LVAD. The apical cuff of the Toyobo was not exchanged because the size was the same as that of the DuraHeart. All conversion operations were performed safely, but 3 patients who had infection of the Toyobo LVAD cannulation site prior to conversion suffered later pocket infections and 1 patient died because of sepsis. One patient underwent heart transplantation and 6 of 8 patients were awaiting heart transplantation at home.

Conclusions: Conversions from the Toyobo LVAD to the DuraHeart LVAD were performed safely. Considering that implantable LVADs provide superior long-term survival and quality of life, conversion is a reasonable decision for Toyobo LVAD users in whom there are no infections. (*Circ J* 2012; **76:** 372–376)

Key Words: Heart failure; Heart-assist device; Surgery

Left ventricular assist devices (LVADs) provide effective bridge-to-transplant therapy for patients with end-stage heart failure and are increasingly used for destination therapy.[1–6] Several types of continuous-flow implantable devices have been developed and have demonstrated significantly improved clinical results with reduction in pump-related morbidity and improvement in both survival length and quality of life (QOL).[7–9] These devices are highly beneficial for patients awaiting heart transplants in Japan, where waiting time exceeds 2 years due to severe donor shortage.

Due to so-called "device lag", however, implantable VADs have not been available in Japan for a long time, and the Toyobo LVAD (Nipro, Osaka, Japan), a paracorporeal pneumatic device, has been the only choice for most patients.[10] As described in previous reports, long-term use of Toyobo LVADs involves serious problems, including not only a high complication rate of stroke and driveline infection but also low QOL due to very limited ambulation.[11,12] Thus, the introduction of new-generation implantable LVADs in Japan, where long-term bridges to transplants are needed, is very important.

Currently, several types of continuous-flow LVADs such as DuraHeart (Terumo Heart, Ann Arbor, MI, USA), HeartMate II (Thoratec Corporation, Pleasanton, CA, USA), Jarvik 2000 (Jarvik Heart, New York, NY, USA), and EVAHEART (Sun Medical, Nagano, Japan) have already approved or are expected to be approved soon in Japan. Of these devices, the DuraHeart is the world's first approved, magnetically levitated centrifugal pump designed for long-term circulatory support. Previous studies found that the DuraHeart was able to provide safe and reliable long-term circulatory support with an improved survival and an acceptable adverse event rate in advanced heart failure patients who were eligible for transplantation.[13,14] Recently, this device was approved by the Japanese Ministry of Health, Labor and Welfare.

Considering the long waiting time for patients who have already undergone implantation with a Toyobo LVAD, we believe conversion to an implantable continuous-flow device provides a safer bridge to transplantation and promises higher QOL. Herein, we report our experience with the conversion of Toyobo LVADs to DuraHeart LVADs in patients awaiting

Received August 1, 2011; revised manuscript received October 17, 2011; accepted October 18, 2011; released online November 27, 2011 Time for primary review: 30 days
Division of Cardiovascular Surgery, Department of Surgery, Osaka University Graduate School of Medicine, Suita, Japan
Grant-in-Aid for Scientific Research, Ministry of Health, Labor and Welfare, Japan.
Mailing address: Yoshiki Sawa, MD, Division of Cardiovascular Surgery, Department of Surgery, Osaka University Graduate School of Medicine, 2-2 Yamada-oka, Suita 565-0871, Japan. E-mail: sawa@surg1.med.osaka-u.ac.jp
ISSN-1346-9843 doi:10.1253/circj.CJ-11-0833

Table 1. Patient Characteristics Prior to Conversion

Patient no.	Sex	Age (years)	BSA	Diagnosis	Before Toyobo support	Purpose of Toyobo	Pre-Toyobo comment	Toyobo duration (days)	Pre-conversion characteristics
1	M	30	1.54	CM	IABP	Bridge to decision	RHF, liver failure	9	Stable
2	M	25	1.51	CM	PCPS	Bridge to decision	RHF, ARF, CHDF	14	Cannula site infection
3	M	26	1.74	CM	IABP	BTT		228	Severe AR, cannula site erosion
4	F	35	1.53	Myocarditis	PCPS	BTT	BiVAD	174 (BiVAD)	Severe PR
5	F	30	1.58	Myocarditis	PCPS	BTT	BiVAD	224 (BiVAD)	Cannula site infection
6	F	34	1.45	CM	PCPS	BTT		268	Stable
7	M	28	1.50	CM	IABP	BTT		335	Stable
8	F	37	1.43	CM	PCPS	BTT		113	Stable

BSA, body surface area (m^2); CM, idiopathic cardiomyopathy; IABP, intraaortic baloon pumping; RHF, right heart failure; PCPS, percutaneous cardiopulmonary support; ARF, acute renal failure; CHDF, continuous hemodialysis and filtration; BTT, bridge to transplantation; AR, aortic regurgitation; BiVAD, biventricular assist device; PR, pulmonary regurgitation.

heart transplantation.

Methods and Results

Patients

Between November 2009 and July 2011, 8 patients underwent conversion to a DuraHeart LVAD at Osaka University Hospital. These patients had no serious organ dysfunction other than the heart or systemic infections, and were expected to receive good family support while awaiting heart transplantation at home. The protocol and documents for patient informed consent were reviewed and approved by the ethics committee at Osaka University Hospital. The operative risks and benefits were shared with the patients and written informed consent was obtained from all the patients. All conversion-related costs were supported by a Grant-in-Aid for scientific research from the Ministry of Health, Labor, and Welfare of Japanese Government.

Eight patients (4 male, 4 female) using Toyobo extracorporeal LVADs underwent conversion to DuraHeart LVADs. Patient characteristics are summarized in Table 1. The median patient age was 30 years (range, 25–37 years) and all patients were on the transplant list. The median duration of Toyobo support was 224 days (range, 9–335 days). Six patients had idiopathic cardiomyopathy (patients 1–3, 6, 7 and 8) and 2 had fulminant myocarditis and had been supported by Toyobo biventricular VADs (BiVAD) for 174 days (patient 4) and 224 days (patient 5), respectively.

There were 2 patients (patients 1 and 2) whose duration of Toyobo support was <2 weeks. Patient 1 underwent emergency implantation with a Toyobo LVAD for acute hemodynamic deterioration. Patient 2 underwent implantation with a Toyobo LVAD at another hospital and was transferred to Osaka University Hospital for the DuraHeart LVAD implantation. Because pre-LVAD evaluation raised a concern about BiVAD requirement due to severe right heart failure and ongoing multi-organ failure, primary implantation of the DuraHeart LVAD was delayed at that time. Conversion to DuraHeart was electively performed following hemodynamic stabilization and improvement of end-organ function with the Toyobo LVAD.

In patients 3 and 4, the conversion was performed because the patients had developed progressive heart failure even with Toyobo support due to severe aortic valve (patient 3) or pulmonary valve (patient 4) insufficiency. Direct aortic/pulmonary valve closures were added to the implantation of the

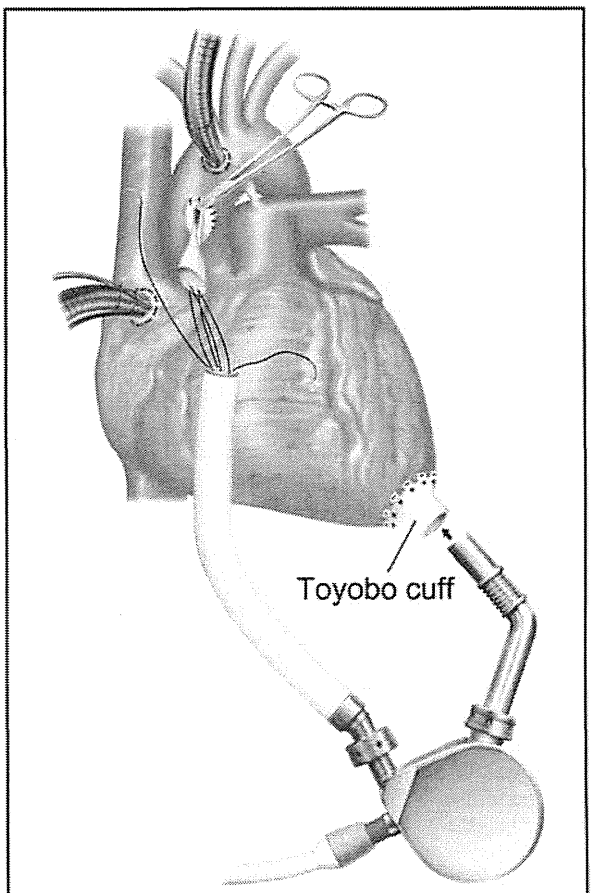

Figure 1. The DuraHeart inflow cannula was inserted into the Toyobo apical cuff, then the Toyobo outflow graft was amputated near the ascending aorta and the DuraHeart outflow graft anastomosed.

Table 2. Operative Procedure and Clinical Outcome

Patient no.	Operation time (min)	CPB time (min)	Cross-clamp time (min)	Concomitant procedure	DuraHeart Duration (days)	Complication	Results
1	278	103	0		631		Ongoing (outpatient)
2	387	81	0		332	Pocket infection	Ongoing (outpatient)
3	498	227	68	AV closure	584	Pocket infection	Ongoing (outpatient)
4	672	255	0	Jarvik2000, PV closure	570		Ongoing (outpatient)
5	565	153	0	Jarvik2000	294	Tracheostomy, pocket infection	Death
6	251	44	0		493	Device exchange	Ongoing (outpatient)
7	344	39	0		176		Transplantation
8	328	60	0		30		Ongoing (outpatient)

CPB, cardiopulmonary bypass; AV, aortic valve.

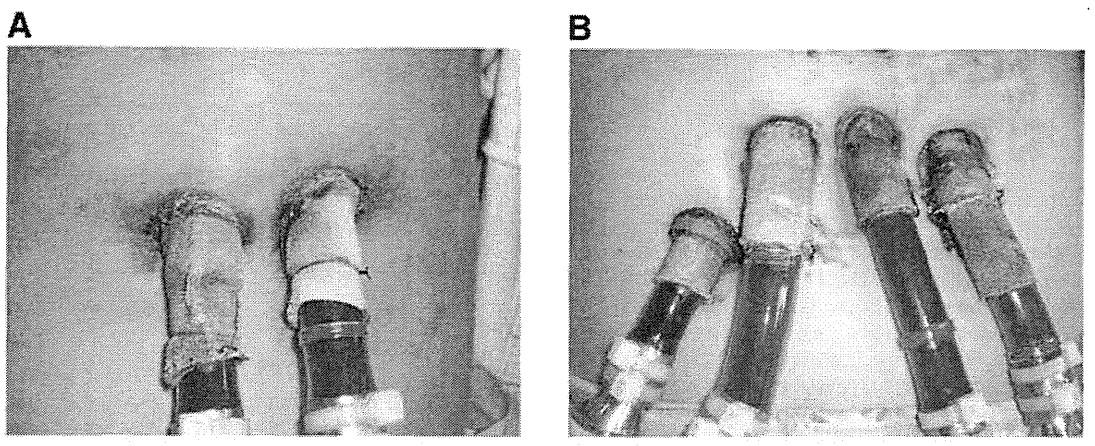

Figure 2. (A) Patient 3 had only minor erosion around the exit site of the Toyobo left ventricular assist device prior to conversion. (B) Patient 5 had methicillin-resistant *Staphylococcus aureus* infection of the Toyobo cannula exit sites.

DuraHeart LVAD.

Having carried out several conversion cases and ensured the safety of the procedure, we extended the indication for conversion to stable patients. Considering the poor long-term results of the Toyobo BiVAD, patient 5 underwent conversion to a DuraHeart LVAD and Jarvik 2000 for right ventricular assist device (RVAD). Patients 6, 7 and 8 experienced no major complications with the Toyobo LVAD during their 224-, 335-, and 113-day support, but it was also anticipated that they would face a wait of >1 year for heart transplantation; conversions were performed with the aim of a safer bridge to transplantation and higher QOL.

Operative Procedure

All operations were performed using a repeat median sternotomy. The heart was dissected and the Toyobo inflow/outflow cannulae were freed. Another skin incision was made vertical to the midline incision across the inflow and outflow cannulae exit site, and the inflow and outflow graft of the Toyobo LVAD were dissected. The skin exit site was trimmed off and the space above the peritoneum was dissected and the left side of the diaphragm was cut at its connection with the anterior chest wall. The DuraHeart pump cable was tunneled s.c. to exit the skin at the left lower quadrant to keep away from the prior cannulation site. After systemic heparinization, a cardiopulmonary bypass (CPB) was initiated with cannulation of the ascending aorta and right atrium. The operative field was flooded with carbon dioxide. The aortic root venting cannula was placed to evacuate residual air. All procedures were performed on a beating heart except in 1 case requiring aortic valve closure (patient 3). The Toyobo inflow cannula was carefully removed from the apical cuff and the left ventricular cavity was inspected. Any mobile wedge thrombi were carefully excised. The Toyobo apical cuff can be used for the DuraHeart device because the sizes of the inflow cannulae of both devices are identical. The sizes of the outflow graft (12 mm) are also the same for both devices. These size similarities make the conversion procedure very easy and safe because the most serious concerns in LVAD implantation procedures are bleeding from the suture line of the apical cuff and from the anastomotic site of the outflow graft. The DuraHeart inflow cannula was inserted into the Toyobo apical cuff and secured with several silk ties. The Toyobo outflow graft was amputated near the ascending aorta and the DuraHeart outflow graft was anastomosed end-to-end using a continuous 4-0 polypropylene suture (Figure 1). The air was then carefully removed, the pump position was adjusted to obtain an optimal flow rate, and CPB was gradually discontinued.

Patient 3 experienced severe aortic insufficiency and developed symptoms of progressive heart failure despite receiving